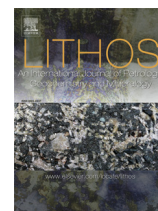




Contents lists available at ScienceDirect

Lithos

journal homepage: www.elsevier.com/locate/lithos

Post-collisional magmatism in the Late Miocene Rodna-Bârgău district (East Carpathians, Romania): Geochemical constraints and petrogenetic models

Lorenzo Fedele ^{a,*}, Ioan Seghedi ^b, Sun-Lin Chung ^{c,d}, Fabio Laiena ^a, Te-Hsien Lin ^d, Vincenzo Morra ^a, Michele Lustrino ^{e,f}

^a Dipartimento di Scienze della Terra, dell'Ambiente e delle Risorse (DiSTAR), Università degli Studi di Napoli Federico II, Via Mezzocannone 8, 80134 Napoli, Italy

^b Institute of Geodynamics, Romanian Academy, 19-21, Jean-Luis Calderon str., Bucharest 020032, Romania

^c Institute of Earth Sciences, Academia Sinica, Taipei 11529, Taiwan

^d Department of Geosciences, National Taiwan University (NTU), Taipei 10617, Taiwan

^e Dipartimento di Scienze della Terra, Università degli Studi di Roma La Sapienza, P.le Aldo Moro 5, 00185 Roma, Italy

^f CNR, Istituto di Geologia Ambientale e Geoingegneria (IGAG), c/o Dipartimento di Scienze della Terra, Università degli Studi di Roma La Sapienza, P.le A. Moro 5, 00185 Roma, Italy

ARTICLE INFO

Article history:

Received 29 July 2016

Accepted 13 October 2016

Available online xxxx

Keywords:

Calcaline magmatism

East Carpathians

Zircon U-Pb dating

Sr-Nd-Hf isotopes

ABSTRACT

Post-collisional magmatism in the Late Miocene Rodna-Bârgău subvolcanic district (East Carpathians) gave rise to a wide variety of rock compositions, allowing recognition of four groups of calcalkaline rocks with distinctive petrography, mineral chemistry, whole-rock geochemistry and Sr-Nd-Hf isotope features. New U-Pb zircon datings, together with literature data, indicate that the emplacement of the four rock groups was basically contemporaneous in the 11.5–8 Ma time span. The low potassium group (LKG) includes the most abundant lithotypes of the area, ranging from basaltic andesite to dacite, characterized by K-poor tschermakitic amphibole, weak enrichment in LILE and LREE, relatively low $^{87}\text{Sr}/^{86}\text{Sr}$, coupled with relatively high $^{143}\text{Nd}/^{144}\text{Nd}$ and $^{176}\text{Hf}/^{177}\text{Hf}$. The high potassium group (HKG) includes amphibole-bearing microgabbro, amphibole andesite and amphibole- and biotite dacite, with K-richer magnesio-hastingsite to hastingsite amphibole, more marked enrichments in incompatible elements, higher $^{87}\text{Sr}/^{86}\text{Sr}$ and lower $^{143}\text{Nd}/^{144}\text{Nd}$ and $^{176}\text{Hf}/^{177}\text{Hf}$. These two main rock groups seem to have originated from similar juxtaposed mantle sources, with the HKG possibly related to slightly more enriched domains (with higher H₂O reflected by the higher modal amphibole) with respect to LKG (with higher plagioclase/amphibole ratios). The evolution of the two rock series involved also open-system processes, taking place mainly in the upper crust for the HKG, in the lower crust for LKG magmas. In addition, limited occurrences of generally younger strongly evolved peraluminous rhyolites and microgranites (Acid group) and sialic-dominated “leucocratic” andesites and dacites (LAD group) were also recognized to the opposite outermost areas of the district. These two latter rock groups were generated by the melting of a basic metamorphic crustal source (respectively in hydrous and anhydrous conditions), favored by the heat released by mantle melts from the adjoining central area. The peculiar distribution of the products of the four rock groups in well defined sectors argues for a strong control of the local crustal tectonic regime on magmatism, influenced by the change from a transpressional to tetrastensional stage.

© 2016 Elsevier B.V. All rights reserved.

1. Introduction

The Alpine-Himalayan Orogen is commonly characterized by a scattered and discontinuous igneous activity, mostly postdating the diachronous continent-continent collisional stages. Such magmatism is generally complex, involving the activation of both mantle and crustal sources (e.g., Lustrino et al., 2011; Prelević and Seghedi, 2013). Despite the wealth of data and interpretations on such widely distributed igneous rocks, a full comprehension of the petrogenetic processes and the

role of crustal lithologies remains controversial. Therefore, detailed petrological investigation on the products of this magmatism can allow better understanding of chemical geodynamics, i.e., the link between physical processes (e.g., oceanic plate subduction and continent-continent collision) and geochemical response of mantle sources, by unraveling the complex interplay between tectonic and magmatic processes.

The Late Miocene Rodna-Bârgău district, as a part of the so-called Eastern Carpathians Subvolcanic Zone (ECSZ), in the East Carpathians range (Fig. 1), offers a good opportunity to apply chemical geodynamics in a post-collisional tectonic setting. Although some of the districts of the Carpathian Arc have been thoroughly investigated (e.g., Kiss et al.,

* Corresponding author.

E-mail address: lofedele@unina.it (L. Fedele).

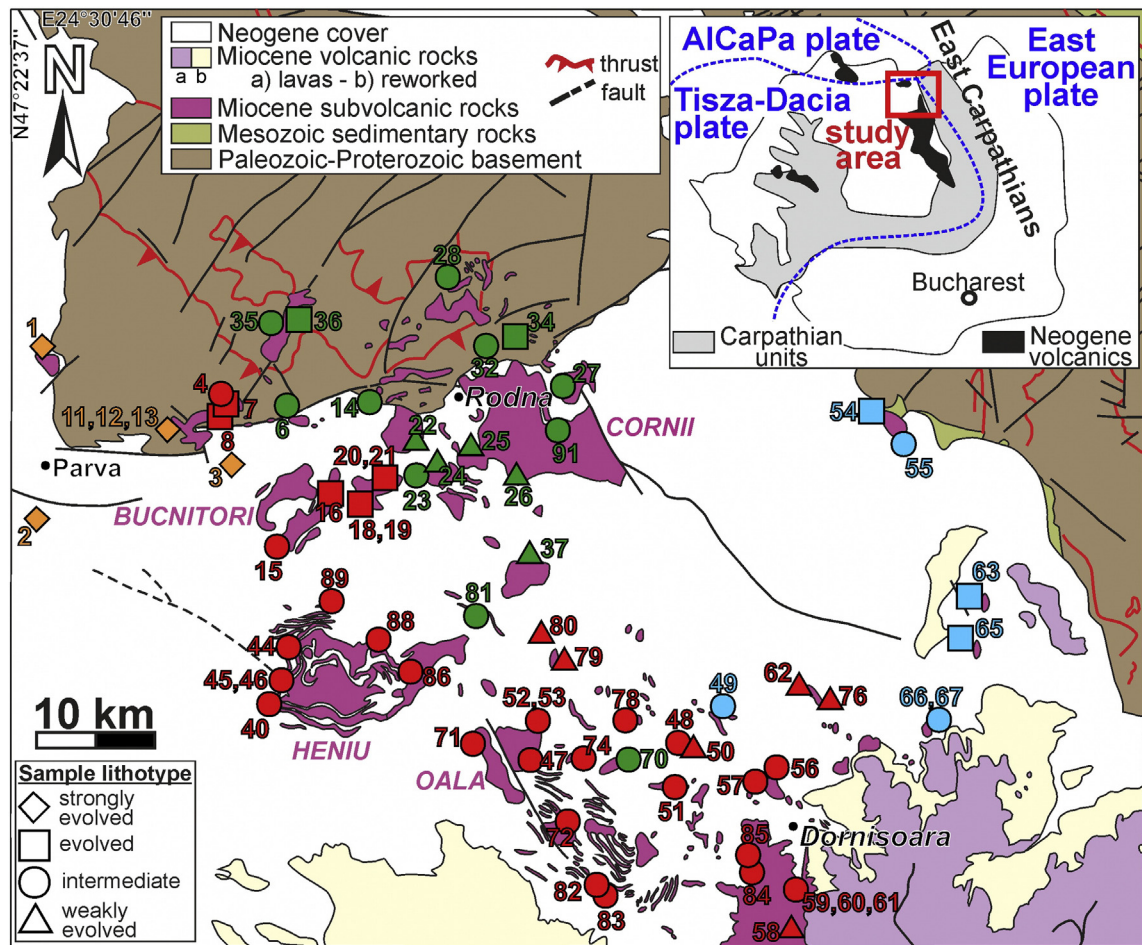


Fig. 1. Geological sketch map of the Rodna-Bârgău subvolcanic district (modified from the *Geological map of Romania, scale 1:200,000, 1967-1969*) with location of the collected samples (only numbers, label FLN was omitted; samples collected not in situ were not included). At the lower right, the neighboring NW portion of the Călimani volcanic complex is also included (after *Seghedi et al., 2005*). Different colors for the sample rock types refer to the four petrochemically-recognized groups (see text for details). The names of the main subvolcanic bodies are reported in purple. The inset shows the position of the district within the framework of the East Carpathians and the outlines of the main lithospheric plates (after *Schmid et al., 2008*). (For interpretation of the references to color in this figure legend, the reader is referred to the web version of this article.)

2014; Mason et al., 1995, 1996, 1998; Seghedi et al., 1995, 2004, 2011), much lesser effort has been so far devoted to the study of the ECSZ (Jurje et al., 2014; Nițoi et al., 2002; Papp et al., 2005). Numerous features make the Rodna-Bârgău a district of potential interest, including: 1) its position at the junction between three lithospheric plates (i.e., East European, Tisza-Dacia and AlCaPa; Schmid et al., 2008); 2) the occurrence of a wide range of igneous rocks and 3) the occurrence of a great variety of enclaves (Nițoi et al., 2002), testifying for complex low-pressure evolution.

In order to shed light on the various post-collisional processes and dynamics that governed the magmatic and tectonic evolution of the Rodna-Bârgău subvolcanic district, a mineralogical, petrochemical, geochronological and isotopic characterization of the occurring lithotypes has been undertaken here. This allows a reevaluation of the petrogenetic processes in this complex key-area and might possibly lead to new progresses in the currently conventional models for the Cenozoic “subduction-related” magmatism of the Mediterranean area (e.g., Harangi et al., 2006; Lustrino et al., 2011).

2. Geological framework

The Carpathian magmatic range is a region that during the Cenozoic was characterized by a complex and not yet fully agreed geodynamic and magmatic history (e.g., Carminati et al., 2012; Seghedi and Downes, 2011). The Carpathians represent an arcuate fold-and-thrust belt with a variable tectonic transport towards N, NE, E, SE and S,

bordered by the Pannonian and Transylvanian basins on the western side. The Pannonian Basin is characterized by a relatively thin lithosphere and crust (50–80 km and 22–30 km, respectively) coupled with high heat flow (>80 mW/m²; see Harangi and Lenkey, 2007 and references therein), while the Transylvanian Basin is characterized by thicker lithosphere and crust (respectively 100–130 km and 30–40 km; Dérerova et al., 2006) and lower surface heat-flux (30–60 mW/m²). The Transylvanian Basin experienced minor Middle Miocene upper crustal extension, and Late Miocene small scale contraction features and shallow salt diapirs (Krézsek and Bally, 2006; Mațenco et al., 2010). The Cenozoic geodynamic evolution of the Carpathian-Pannonian area is related to the W-SW-S-directed subduction of a small oceanic (or thinned-continental) embayment (Carpathian Embayment), followed by a continent-continent collision occurred along southwestern margin of the East European plate. Such subduction was probably the consequence of the lateral expulsion of the Southern Alps following the collision with the northern margin of the Adriatic microplate (e.g., Carminati et al., 2012; Csontos et al., 1992; Handy et al., 2010).

Magmatic activity in the East Carpathians can be subdivided into three stages: 1) an Early-Middle Miocene phase, with emplacement of acid calcalkaline tuffs and ignimbrites (Lukács et al., 2015; Szakács et al., 2012), 2) a Middle Miocene to Pliocene phase, characterized by mainly intermediate calcalkaline lavas and subvolcanic bodies (Seghedi et al., 2004) and 3) a Plio-Pleistocene phase, with eruption of adakite-like and K- and Na-alkaline lavas in the southeastern-most tip

of the arc (Eastern Transylvanian Basin, ETB; Mason et al., 1998; Seghedi et al., 2011). The calcalkaline magmas are thought to have originated from a mantle source contaminated by subduction-related metasomatic agents (Harangi and Lenkey, 2007; Seghedi et al., 2004). Adakite-like magmatism (in the South Harghita district) was interpreted as the result of a corner-flow around the steepening and melting slab, plus differentiation within the lower crust (Seghedi and Downes, 2011). This process was coeval with the slab tearing, whereas the sodic mildly alkaline “anorogenic” magmatism was triggered by asthenospheric passive upwelling during slab sinking (Harangi et al., 2013; Seghedi et al., 2011).

2.1. The Rodna-Bârgău subvolcanic district

The Late Miocene Rodna-Bârgău subvolcanic district is located in the internal part of the East Carpathians (northern Romania), including terranes belonging to the northeastern part of the Tisza mega-unit (Biharia unit) and to the northern part of the Dacia mega-unit (Bucovinian nappes; Săndulescu, 1994; Fig. 1). According to Tischler et al. (2007), the tectonic contacts between the two mega units (commonly referred to as a single tectonic block) and the remnants of an interposed ocean domain are unconformably sealed by Late Cretaceous-Paleocene (conglomerates, sandstones and marls) and Eocene-Burdigalian (conglomerates, carbonates, marls and turbidites) sedimentary covers. During the final stages of the closure of the Carpathian embayment, the Bucovinian nappes were emplaced above the Cretaceous-Miocene flysch deposits presently forming the Miocene fold-and-thrust belt of the eastern Carpathians (Maţenco and Bertotti, 2000). During the Burdigalian, the Tisza and Dacia mega-units, together with their Eocene-Burdigalian sedimentary cover, were overthrust by the “Pienides” flysch nappes of the easternmost part of the AlCaPa (Alps-Carpathians-Pannonian) mega-unit. At the end of Burdigalian, the rotation of Tisza-Dacia during convergence with AlCaPa resulted in a migration of shortening and extension (Tischler et al., 2008).

The most important tectonic element present in the Rodna-Bârgău area is the E-W-striking Bogdan-Dragoş-Vodă fault system that, according to Tischler et al. (2007, 2008) and Gröger et al. (2008), records compressive (from 20.5 to 18.5 Ma), extensional (18.5–16 Ma) and eventually sinistral transpressional (16–12 Ma) and transtensional deformation stages (12–10 Ma). To the West, the Bogdan-Dragoş-Vodă fault system offsets the Eocene-Burdigalian deposits covering the Tisza and Dacia mega-units and the Pienides nappes (Tischler et al., 2007). To the East, the main fault system forms the northern boundary of the Rodna horst crystalline body. Magma upwelling and emplacement were favored by the 12–10 Ma transtensional stage (Pécskay et al., 2009; Seghedi and Downes, 2011; Tischler et al., 2007). The transtensional deformation stage is thought to be the consequence of the oblique convergence of the AlCaPa and Tisza-Dacia blocks with the NW-SE striking European margin, evidenced by eastward thrusting in the external Miocene thrust belt (Maţenco and Bertotti, 2000). Blocking of the Tisza-Dacia eastward movement in the North led to sinistral strike-slip activity along E-W trending faults and coeval normal faulting along NE-SW and NW-SE directions (Gröger et al., 2008; Tischler et al., 2007).

The subvolcanic rocks of the Late Miocene Rodna-Bârgău district were emplaced within the Dacia mega-unit between 11.4 and 8.0 Ma (K-Ar dating, Pécskay et al., 2009), forming, together with the Poiana-Botizei-Țibleş-Toroiaga districts, the East Carpathians Subvolcanic Zone (ECSZ). These districts are interposed between the two mainly volcanic districts of Oaş-Gutâi (to the NW) and Călimani-Gurghiu-Harghita (to the SE; e.g., Seghedi et al., 2004; Fig. 1), defining a linear array parallel to the eastern Carpathian Belt, with emplacement ages decreasing from NW to SE, most evident along Călimani-Gurghiu-Harghita chain (Pécskay et al., 1995, 2006).

The shallow level intrusions of the Rodna-Bârgău district form a clear NW-SE alignment and are hosted within metamorphic rocks

of the Rodna horst (mainly garnet-bearing micaschists, paragneisses and amphibolites) to the North, within the Cretaceous-Paleogene sedimentary rocks to the South (conglomerates, limestones, marls, sandstones and argillaceous marls; e.g., Niţoi et al., 2002; Papp et al., 2005; Fig. 1). The contact zones between magmatic rocks and sedimentary host-rocks are often marked by hornfelses and, less frequently, breccias (Pécskay et al., 2009). The intrusions crop out in the form of laccoliths, sills, stocks and dykes (Niţoi et al., 2002; Papp et al., 2005; Peltz et al., 1972), possibly representing magma chambers that fed subaerial volcanism (Seghedi and Downes, 2011), their exposure being related to the strong erosion during the uplift of Rodna horst system (Gröger et al., 2008). The largest subvolcanic bodies (Cornii, Heniu and Oala), hosted in sedimentary rocks close to kilometric faults, are usually surrounded by swarms of dykes and smaller bodies (Fig. 1; Pécskay et al., 2009).

3. Sampling and analytical techniques

A detailed sampling of magmatic products cropping out in the Rodna-Bârgău district has been undertaken during this study (Fig. 1). Incomplete exposure and vegetation cover usually hamper a clear size estimation of the subvolcanic bodies, which approximately cover an area ranging from few tens up to several hundreds of m². Many of the shallow intrusions commonly host a wide variety of enclaves (i.e., magmatic cognate inclusions, as well as metamorphic, igneous, sedimentary xenocrysts and xenoliths; Niţoi et al., 2002), ranging from few centimeters up to ~25 cm in size. Rocks are generally massive (flow structures are only rarely observed), strongly fractured and often display the effects of a variable weathering. The exposure conditions are generally better with respect to the other districts of the ECVZ, where magmatic rocks commonly display evidence of extensive argillic and propylitic alteration, associated with Cu-Pb mineralizations (Pécskay et al., 2009).

A total of 99 samples has been collected from all the main subvolcanic bodies (plus some from the smaller ones), processed and analyzed for petrochemical characterization at the DiSTAR laboratories. Samples were crushed, washed in deionized water, dried out and then pulverized in a low-blank agate mill in order to obtain pressed powder pellets analyzed for major- and trace elements by XRF (X-ray fluorescence) spectrometry using a Panalytical Axios instrument. Analytical uncertainties are in the order of 1–2% for major elements and 5–10% for trace elements. Weight loss on ignition (LOI) was determined gravimetrically after heating rock powders (pre-dried at ~150 °C overnight) at 950 °C for 4 h. Whole rock samples with LOI >4 wt.% were not taken into account in the petrochemical discussion. Composition of the main mineral phases was analyzed for a selection of 11 representative samples by EDS (energy dispersive spectrometry) using an Oxford Instruments Microanalysis Unit equipped with an INCA X-act detector and a JEOL JSM-5310 microscope. Measurements were performed with an INCA X-stream pulse processor using a 15 kV primary beam voltage, 50–100 µA filament current, variable spot sizes and 50 s of acquisition time. Standards for calibration were diopside (Mg), wollastonite (Ca), anorthoclase (Al and Si), albite (Na), rutile (Ti), almandine (Fe), Cr₂O₃ (Cr), rhodonite (Mn), orthoclase (K), apatite (P), fluorite (F), barite (Ba), strontianite (Sr), zircon (Zr and Hf), ilmenite (Nb), synthetic Smithsonian orthophosphates (La, Ce, Nd, Sm and Y), pure vanadium (V), Corning glass (Th and U), sphalerite (S and Zn), sodium chloride (Cl) and pollucite (Cs). Relative analytical uncertainty is typically ~1–2% for major elements, ~3–5% for minor elements. The results are reported in the tables of the Electronic Supplementary Material 1.

In addition, ICP-MS (Inductively-Coupled Plasma Mass Spectrometry) analyses for trace element concentrations were performed at ActLabs (Ontario, Canada) on a selection of 39 representative samples (see www.actlabs.com for full analytical details). Among these samples, 14 were selected for Sr-Nd-Hf isotope analyses performed at the Shensu Sun Memorial Lab of the Department of Geosciences, NTU. Sample

preparation was carried out in a clean room where Sr, Nd and Hf were purified via column separation and then isotope ratios were measured using a Finnigan-Thermo Neptune® multiple collector mass spectrometer (MC-ICP-MS). The procedures were described in Lee et al. (2012) and Shinjo et al. (2010) for Sr–Nd and Hf isotopes, respectively. In addition, seven selected intermediate and evolved rock samples were chosen for zircon U–Pb age determinations. Separated zircon crystals were incorporated in an epoxy resin plug and polished. Then cathodoluminescence (CL) images were taken with a SEM at the Institute of Earth Sciences, Academia Sinica (Taipei) to select suitable sites for analyses. These were performed by laser ablation–ICP–MS (LA–ICP–MS) using an Agilent 7500 s quadrupole instrument and a New Wave UP213 system housed at NTU. All U–Th–Pb isotope ratios were calculated using the GLITTER version 4.4 (GEMOC) software and common lead was corrected following Andersen (2002). The weighted mean U–Pb ages and concordia plots were obtained using the Isoplot version 3.75 software. Full details on operating conditions and data acquisition parameters are in Chiu et al. (2009).

4. Results

4.1. Petrography and mineral chemistry

The igneous rocks from the Rodna–Bârgău district display a wide range of compositions, from relatively weakly evolved rocks up to strongly evolved ones. Below only the most relevant features of each lithotype are reported. A detailed description is provided in the Electronic Supplementary Material 2.

Weakly evolved rocks are represented by two lithotypes: *amphibole microgabbro* (Amph–mGb) and *amphibole- and clinopyroxene-basaltic andesite* (Amph + cpx–bA). The first is characterized by ~50:50 plagioclase:mafic minerals (green amphibole and clinopyroxene) ratio, plus occasional biotite and alkali feldspar. The second lithotype is dominated by plagioclase phenocrysts, with less abundant yellow to brown amphibole and clinopyroxene. Both display a roughly normal zoned plagioclase with wide compositional variation (respectively $An_{36-88}Ab_{12-62}Or_{0-5}$ and $An_{55-83}Ab_{12-45}Or_{0-1}$) and a diopside-augite clinopyroxene ($Mg\# = 0.64-0.85$ and $0.68-0.83$), whereas amphiboles are clearly different in terms of K content ($0.10-0.19$ apfu for Amph–mGb, $0.03-0.09$ for Amph + cpx–bA).

Intermediate rocks include three lithotypes: *amphibole andesite* (Amph–A), *plagioclase andesite* (Pl–A) and *leucocratic andesite* (Leuco–A). The first is mainly characterized by green amphibole and plagioclase phenocrysts (plus sporadic biotite, clinopyroxene and alkali feldspar), whereas the second (the most abundant rock type of the entire area) is dominated by plagioclase plus lesser amphibole and clinopyroxene. The two rock types display distinctive amphibole compositions, with Amph–A showing a magnesio-hastingsite K-rich composition ($K = 0.16-0.34$ apfu), while Pl–A has tschermakite/magnesio-hastingsite K-poor composition ($K = 0.01-0.07$ apfu). The Leuco–A is a very subordinate variety dominated by plagioclase phenocrysts with very rare alkali feldspar, quartz, amphibole (K-poor tschermakite with $K < 0.1$ apfu) and groundmass clinopyroxene and orthopyroxene (both Fe-rich, with $Mg\# = 0.52-0.53$ and $0.46-0.52$, respectively).

Evolved rocks include *amphibole- and biotite-dacite* (Amph + bt–D), *amphibole dacite* (Amph–D) and *leucocratic dacite* (Leuco–D). The first is characterized by plagioclase, green amphibole and alkali feldspar plus lesser quartz and biotite phenocrysts, whereas the second has plagioclase, green amphibole, quartz and subordinate alkali feldspar. The main differences in terms of phase composition are again displayed by amphiboles. The Amph + bt–D has K-richer varieties with respect to Amph–D ($0.21-0.37$ vs. $0.04-0.09$ apfu), which also includes both a ^{VI}Al -richer, Mg- and Ca-poorer and a ^{VI}Al -poorer, Mg- and Ca-richer subgroups. The very rare Leuco–D is made of plagioclase, quartz, alkali feldspar and very rare green ferro-tschermakite amphibole, biotite and Fe-rich groundmass orthopyroxene ($Mg\# = 0.33-0.38$).

Strongly evolved acid rocks are mainly represented by *rhyolite* (Rhy), made of alkali feldspar, quartz and plagioclase phenocrysts, plus very rare Al-rich biotite ($Al_2O_3 = 17.8-18.7$ wt.%), amphibole and muscovite.

4.2. Whole rock major and trace element geochemistry

Following Miyashiro (1974) and Arculus (2003), the majority of the Rodna–Bârgău igneous rocks fall in the fields for calcalkaline or Low-Fe subalkaline series (Fig. 2). However, based on the TAS diagram and, even more evidently, on K_2O contents, two main groups can be recognized: 1) a low-K group (LKG, red symbols in Fig. 2), including Amph + cpx–bA, Pl–A and Amph–D, with K_2O ranging from 0.56 to 1.64 wt.% and 2) a high-K group (HKG, green symbols), including Amph–mGb, Amph–A and Amph + bt–D, with K_2O in the range of 1.27–3.36 wt.% (Figs. 2 and 3). Rocks of these two main groups largely overlap in composition for most of the major and trace elements (Tables 1 and 2), although the LKG rocks reach slightly higher silica contents. Both HKG and LKG rocks are characterized by strong decrease of TiO_2 , Fe_2O_3 tot, MgO, CaO, Sc, V and Cr and increase of SiO_2 , Na_2O , K_2O , Ba, Sr, Rb and Nb with increasing degree of rock evolution (Fig. 3). The HKG rocks can be distinguished from LKG ones for their higher K_2O , Ba ($382-850$ vs. $106-364$ ppm) and Rb ($44-121$ vs. $11-50$ ppm). Some further differences are observed for the evolved rocks of the two groups, with Y and Zr depicting a decreasing evolutionary trend for LKG dacites, whereas HKG dacites plot on a trend of increasing contents for both elements. Both intermediate and evolved rocks of the LKG have generally higher Al_2O_3 when compared with their counterparts of the HKG.

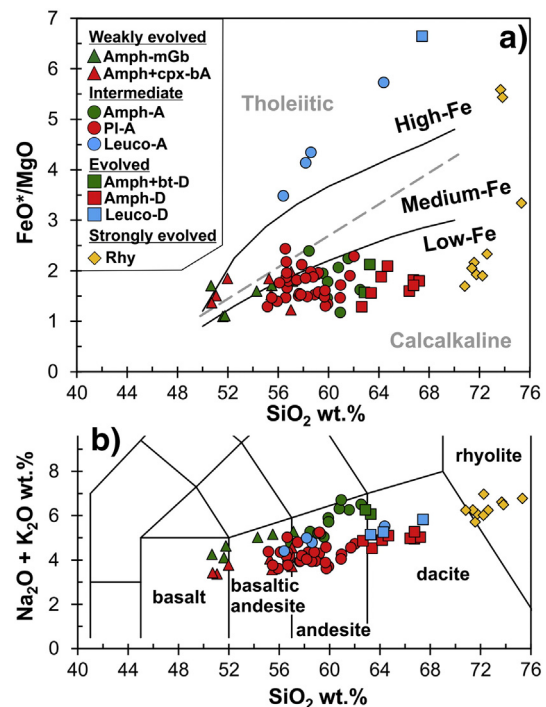


Fig. 2. Classification plots for the analyzed Rodna–Bârgău igneous rocks according to the a) TAS (Le Maitre, 2005) and b) FeO^*/MgO vs. SiO_2 diagrams. In b) thick black lines separate High-Fe, Medium-Fe and Low-Fe series according to Arculus (2003), gray dashed line separates tholeiitic and calcalkaline series after Miyashiro (1974). Different colors for the sample rock types refer to the four petrochemically-recognized groups (see text for details). Amph–mGb = amphibole microgabbro; Amph + cpx–bA = amphibole- and clinopyroxene-basaltic andesite; Amph–A = amphibole andesite; Pl–A = plagioclase andesite; Leuco–A = leucocratic andesite; Amph + bt–D = amphibole- and biotite-dacite; Amph–D = amphibole dacite; Leuco–D = leucocratic dacite; Rhy = rhyolite. (For interpretation of the references to color in this figure legend, the reader is referred to the web version of this article.)

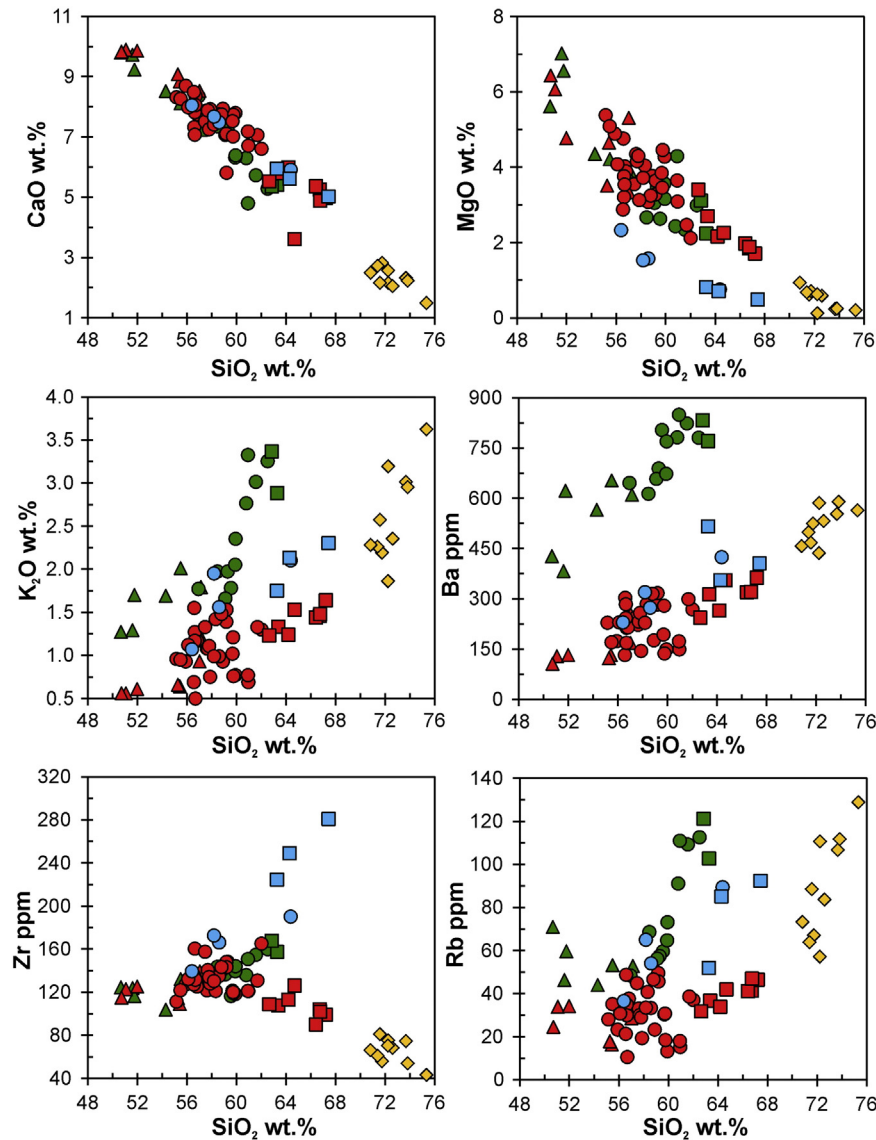


Fig. 3. Selected binary variation diagrams for the analyzed Rodna-Bârgău igneous rocks. Symbols as in Fig. 2.

The Leuco-A and Leuco-D have remarkably high Fe content (thus falling in the fields for tholeiitic and High-Fe subalkaline series) as well as alkali and K_2O contents that are intermediate between those of LKG and HKG rocks. Considering also their peculiar petrography dominated by silic minerals, they are considered to represent a separated “leucocratic andesite and dacite” group (LAD, sky blue symbols). Though showing overall identical evolutionary trends, the intermediate to evolved rocks of the LAD group plot clearly apart from both LKG and HKG counterparts due to their lower MgO (2.33–0.49 wt.%) and higher Zr (140–281 ppm, increasing with magma evolution).

Finally, the strongly evolved rocks set clearly aside in the silica-richest end of the plots, defining an “Acid” group (orange diamond symbols). Rocks of this group display a strongly evolved composition with very high SiO_2 (70.8–75.3 wt.%), and low TiO_2 , $Fe_2O_{3,tot}$, MgO, CaO, V, Y and Zr. They typically plot as a continuation of the evolutionary trends depicted by the LKG rocks and show a clear peraluminous character [$A/CNK = \text{molar } Al_2O_3 / (CaO + Na_2O + K_2O) = 1.15\text{--}1.53$] which is also reflected by the presence of Al-rich biotite (i.e., with high siderophyllite component) and muscovite.

Primitive mantle-normalized diagrams for the least evolved rocks display the typical features of igneous rocks emplaced along active margins, such as high LILE/HFSE (Large Ion Lithophile Elements/High

Field Strength Elements) and HFSE troughs (Ta, Nb, Ti), as well as peaks at Pb and K and, less evidently, at Sr and U (Fig. 4). With respect to LKG rocks, HKG samples have higher LILE/HFSE ratios (e.g., $Ba/Nb = 59.8\text{--}157$ vs. $20.5\text{--}53.6$, $Rb/Nb = 5.67\text{--}12.9$ vs. $2.83\text{--}7.00$, $Ba/Zr = 3.99\text{--}7.14$ vs. $1.12\text{--}2.91$, $Rb/Zr = 0.38\text{--}0.72$ vs. $0.15\text{--}0.42$) and more fractionated REE patterns [Rare Earth Elements; e.g., $La_N/Yb_N = 5.89\text{--}8.56$ vs. $1.83\text{--}4.18$, $La_N/Sm_N = 2.58\text{--}3.34$ vs. $1.34\text{--}2.51$; abundances normalized to the chondrite of Sun and McDonough (1989)]. Intermediate and evolved rocks basically show the same patterns though displaced to progressively higher normalized abundances, a slightly stronger light REE (LREE) enrichment ($La_N/Yb_N = 7.53\text{--}11.7$ and $3.01\text{--}7.74$, $La_N/Sm_N = 3.49\text{--}4.21$ vs. $2.01\text{--}3.61$, respectively for the rocks of HKG and LKG) plus a small peak at Zr and a deeper trough at Ti. In addition, whereas the andesite-dacite transition in the HKG is characterized by the appearance of a small peak at Zr and an overall enrichment also for the heavy REE (HREE), in the LKG it is marked by a slight but clear decrease of Pb, Zr, Hf, Y and HREE. LAD group rocks typically plot between the andesites and dacites of the LKG and the more evolved counterparts of the HKG and show a much more pronounced Zr peak. Rock of the Acid group are those displaying the strongest enrichment in incompatible elements (though comparable with that of the HKG

Table 1

XRF major- and trace element concentrations (respectively in wt.% recalculated to 100% on a water-free basis, and in ppm) for a representative selection of the analyzed Rodna-Bărgău igneous rocks. The full dataset is reported in the Electronic Supplementary Material 1.

Sample	FLN37	FLN26	FLN14	FLN81	FLN34	FLN76	FLN50	FLN79	FLN47	FLN40a	FLN45	FLN83	FLN7	FLN18	FLN55	FLN63b	FLN1	FLN10a	FLN12	FLN2	
Rock	Amph-mGb		Amph-A		Amph + bt-D	Amph-cpx-bA			Pl-A		Amph-D			Leuco-A	Leuco-D	Rhy					
Group	HKG					LKG										LAD		Acid			
SiO ₂	51.76	55.49	60.77	59.89	63.26	51.97	57.01	55.43	56.58	56.63	59.66	61.69	63.37	66.72	58.59	67.42	72.25	71.56	72.59	75.33	
TiO ₂	0.72	0.88	0.63	0.64	0.60	1.03	0.75	0.79	0.80	0.89	0.60	0.50	0.53	0.36	0.75	0.36	0.08	0.11	0.10	0.04	
Al ₂ O ₃	18.68	17.79	17.58	17.53	16.81	18.47	17.13	18.52	18.00	18.37	17.82	18.22	18.09	16.86	18.66	16.99	16.62	18.13	16.65	15.26	
Fe ₂ O ₃ tot	8.09	8.01	5.59	5.81	5.30	9.80	7.24	7.90	7.78	7.83	6.36	5.23	4.70	3.74	7.64	3.62	1.62	1.49	1.53	0.78	
MnO	0.14	0.12	0.15	0.15	0.11	0.18	0.13	0.16	0.15	0.17	0.13	0.11	0.11	0.11	0.20	0.10	0.09	0.08	0.12	0.06	
MgO	6.56	4.22	2.43	3.58	2.24	4.77	5.31	4.65	4.77	3.76	3.85	2.47	2.70	1.85	1.58	0.49	0.13	0.62	0.59	0.21	
CaO	9.23	8.11	6.30	6.32	5.42	9.86	8.53	8.84	7.33	7.82	7.53	7.07	5.80	5.25	7.49	5.03	2.15	2.16	2.05	1.49	
Na ₂ O	2.93	3.15	3.55	3.85	3.19	3.16	2.78	2.93	2.80	3.08	2.87	3.23	3.20	3.50	3.23	3.52	3.77	3.14	3.89	3.15	
K ₂ O	1.70	2.01	2.76	2.05	2.89	0.61	0.93	0.64	1.55	1.27	1.02	1.33	1.33	1.46	1.56	2.30	3.19	2.57	2.35	3.62	
P ₂ O ₅	0.18	0.22	0.23	0.19	0.18	0.14	0.19	0.14	0.24	0.18	0.15	0.15	0.17	0.13	0.29	0.16	0.09	0.13	0.12	0.06	
LOI	2.50	2.26	0.99	2.36	1.30	3.28	2.68	3.56	2.79	2.50	2.31	3.26	2.72	1.73	1.85	1.44	1.26	3.07	1.37	1.55	
Mg#	0.65	0.55	0.50	0.58	0.49	0.53	0.63	0.57	0.58	0.52	0.58	0.52	0.57	0.53	0.32	0.23	0.15	0.48	0.45	0.36	
A/CNK	0.80	0.80	0.87	0.87	0.92	0.78	0.81	0.86	0.92	0.89	0.91	0.93	1.05	1.00	0.90	0.97	1.22	1.53	1.31	1.29	
Sc	24	25	14	16	16	30	23	29	25	21	18	15	17	11	18	9	3	6	5	4	
V	205	263	162	168	158	210	152	190	193	101	132	95	117	82	69	3	23	6	10	17	
Ba	622	653	782	673	772	132	169	132	303	285	194	299	314	321	274	406	586	468	532	564	
Sr	391	363	418	324	402	275	269	236	373	292	263	320	321	280	345	339	276	209	220	153	
Y	18	20	25	20	25	26	21	23	25	27	20	18	20	17	32	28	11	15	11	9	
Zr	117	132	136	140	158	125	131	109	135	161	122	131	108	104	166	281	75	81	68	43	
Cr	53	30	22	37	36	64	85	47	18	35	61	38	46	21	21	14	4	15	11	1	
Ni	22	12	6	11	9	19	31	22	10	14	24	13	11	3	6	4	bdl	6	6	1	
Rb	60	53	91	65	103	34	29	16	49	35	30	39	37	41	54	92	111	89	84	129	
Nb	6	7	9	9	11	9	6	6	9	15	8	8	11	11	9	13	16	12	11	15	

LOI = loss on ignition (wt.%); Mg# = molar Mg/(Fe_{tot} + Mg + Mn); A/CNK = molar Al₂O₃/(CaO + Na₂O + K₂O); Amph-mGb = amphibole microgabbro; Amph-A = amphibole andesite; Amph + bt-D = amphibole- and biotite-dacite; Amph + cpx-bA = amphibole- and clinopyroxene-basaltic andesite; Pl-A = plagioclase andesite; Amph-D = amphibole dacite; Leuco-A = leucocratic andesite; Leuco-D = leucocratic dacite; HKG = high-K group; LKG = low-K group; LAD = leucocratic andesite and dacite group; Acid = acid rocks group.

Table 2
ICP-MS trace element concentrations (in ppm) and Sr-Nd-Hf isotope compositions (measured values, with respective errors at 2σ level) for a representative selection of the analyzed Rodna-Bărgău igneous rocks. The full dataset is reported in the Electronic Supplementary Material 1.

Sample	FLN37	FLN26	FLN14	FLN81	FLN34	FLN76	FLN50	FLN79	FLN47	FLN40a	FLN45	FLN83	FLN7	FLN18	FLN55	FLN63b	FLN1	FLN10a	FLN12	FLN2
Rock	Amph-mGb		Amph-A		Amph + bt-D	Amph-cpx-bA			Pl-A			Amph-D		Leuco-A	Leuco-D	Rhy				
Group	HKG					LKG							LAD		Acid					
Sc	27.0	21.0	11.0	13.0	13.0	26.0	20.0	24.0	16.0	16.0	14.0	9.0	11.0	8.0	9.0	2.0	2.0	3.0	4.0	2.0
V	235.0	227.0	126.0	126.0	114.0	216.0	146.0	191.0	160.0	146.0	111.0	83.0	87.0	60.0	55.0	9.0	7.0	9.0	13.0	bdl
Ba	603.0	631.0	765.0	659.0	767.0	120.0	158.0	103.0	286.0	246.0	170.0	268.0	285.0	314.0	248.0	391.0	619.0	413.0	512.0	568.0
Sr	368.0	369.0	422.0	334.0	404.0	267.0	261.0	238.0	363.0	281.0	250.0	317.0	317.0	287.0	358.0	359.0	283.0	286.0	214.0	184.0
Y	15.0	18.0	22.0	16.0	21.0	20.0	17.0	18.0	21.0	21.0	16.0	13.0	17.0	15.0	26.0	24.0	8.0	12.0	9.0	8.0
Zr	83.0	107.0	132.0	136.0	150.0	91.0	101.0	92.0	120.0	136.0	107.0	122.0	110.0	108.0	162.0	260.0	58.0	60.0	54.0	38.0
Cr	30.0	bdl	bdl	40.0	bdl	50.0	80.0	40.0	bdl	20.0	50.0	20.0	30.0	bdl	bdl	bdl	bdl	bdl	bdl	bdl
Ni	bdl	bdl	bdl	bdl	bdl	bdl	20.0	bdl	bdl	bdl	bdl	bdl	bdl	bdl	bdl	bdl	bdl	bdl	bdl	bdl
Rb	49.0	54.0	90.0	64.0	99.0	21.0	27.0	14.0	46.0	34.0	30.0	32.0	38.0	45.0	46.0	78.0	107.0	72.0	77.0	128.0
Nb	4.0	6.0	7.0	6.0	9.0	4.0	4.0	3.0	7.0	12.0	6.0	5.0	9.0	9.0	6.0	8.0	15.0	7.0	9.0	12.0
Cs	2.1	1.9	3.5	1.8	3.0	3.5	1.0	1.0	1.1	1.0	0.6	0.8	1.6	0.6	4.2	4.1	3.0	7.3	2.5	4.4
La	17.9	21.7	27.4	21.2	26.3	6.4	10.5	5.1	16.7	15.4	10.2	12.0	11.7	15.1	16.4	26.0	29.3	19.8	18.0	22.8
Ce	34.7	41.9	51.6	40.6	51.5	15.2	21.5	12.5	33.5	31.5	21.2	24.9	23.2	30.5	36.6	55.1	52.4	39.8	36.3	33.6
Pr	4.3	5.0	6.1	4.7	6.0	2.1	2.7	1.8	4.1	3.9	2.7	2.9	3.0	3.7	4.5	6.2	5.5	4.6	4.0	4.8
Nd	16.4	19.1	22.9	18.1	23.2	10.0	11.3	8.4	16.4	15.1	10.9	12.3	13.1	13.5	20.0	25.0	18.2	16.5	13.9	16.5
Sm	3.5	4.2	4.4	3.6	4.7	2.9	2.7	2.4	3.6	3.3	2.4	2.6	2.8	2.7	4.4	4.8	3.1	2.9	2.4	3.4
Eu	1.0	1.1	1.2	1.0	1.2	1.0	0.8	0.8	1.0	1.1	0.8	0.8	0.9	0.8	1.2	1.3	0.7	0.6	0.6	0.7
Gd	3.1	3.5	3.9	3.0	4.0	3.1	2.7	2.6	3.4	3.6	2.7	2.1	2.9	2.5	4.2	4.2	2.2	2.3	1.6	2.7
Tb	0.5	0.5	0.6	0.5	0.6	0.5	0.4	0.5	0.6	0.6	0.4	0.4	0.5	0.4	0.7	0.7	0.3	0.3	0.2	0.4
Dy	2.8	3.1	3.5	3.0	3.8	3.4	2.8	3.0	3.6	3.7	2.6	2.1	2.8	2.3	4.2	3.8	1.4	1.7	1.3	1.8
Ho	0.5	0.6	0.7	0.6	0.7	0.7	0.6	0.6	0.7	0.8	0.5	0.4	0.6	0.5	0.8	0.7	0.2	0.3	0.2	0.2
Er	1.6	1.8	2.0	1.8	2.2	2.1	1.7	1.8	2.2	2.2	1.6	1.3	1.6	1.3	2.5	2.0	0.6	0.9	0.7	0.5
Tm	0.2	0.3	0.3	0.3	0.3	0.3	0.3	0.3	0.3	0.4	0.2	0.2	0.3	0.2	0.4	0.3	0.1	0.1	0.1	0.1
Yb	1.5	1.9	2.2	1.8	2.2	2.1	1.8	2.0	2.3	2.4	1.7	1.5	1.8	1.4	2.8	2.2	0.5	0.8	0.6	0.3
Lu	0.2	0.3	0.3	0.3	0.3	0.3	0.3	0.3	0.3	0.3	0.2	0.2	0.2	0.2	0.4	0.4	0.1	0.1	0.1	bdl
Hf	2.1	2.8	3.3	3.0	3.8	1.9	2.6	1.8	2.8	3.0	2.5	2.2	2.7	2.5	3.1	4.6	1.8	1.5	1.6	1.4
Ta	0.4	0.4	0.5	0.6	1.6	0.3	0.3	0.2	0.5	0.8	0.4	0.4	0.7	0.8	0.4	0.7	1.3	0.8	0.8	1.9
Tl	0.2	0.2	0.4	0.3	0.5	bdl	0.1	bdl	0.1	0.1	bdl	0.2	0.2	0.2	0.2	0.5	0.5	0.3	0.3	0.5
Pb	17.0	13.0	19.0	15.0	18.0	bdl	7.0	bdl	10.0	bdl	bdl	10.0	bdl	7.0	8.0	19.0	22.0	9.0	11.0	30.0
Th	5.7	6.4	9.1	6.8	8.5	1.1	2.5	0.8	4.2	3.2	2.3	2.7	2.5	3.7	3.8	6.4	9.8	5.9	5.6	6.4
U	2.0	2.1	3.0	2.7	3.3	0.5	0.9	0.4	1.4	1.0	0.8	1.2	1.0	1.4	1.5	2.2	3.2	1.7	1.9	3.9
⁸⁷ Sr/ ⁸⁶ Sr	0.708427		0.708423	0.708039	0.709564	0.706459		0.705494	0.705831	0.706607		0.705707	0.707240	0.708718	0.709256		0.706947	0.709099		
2σ	0.000012		0.000010	0.000004	0.000009	0.000010		0.000012	0.000008	0.000008		0.000010	0.000010	0.000011	0.000010		0.000010	0.000009		
¹⁴³ Nd/ ¹⁴⁴ Nd	0.512517		0.512494	0.512596	0.512427	0.512746		0.512805	0.512668	0.512618		0.512683	0.512520	0.512461	0.512379		0.512495	0.512351		
2σ	0.000002		0.000002	0.000002	0.000002	0.000003		0.000003	0.000002	0.000003		0.000002	0.000002	0.000002	0.000002		0.000003	0.000002		
¹⁷⁶ Hf/ ¹⁷⁷ Hf	0.282814		0.282811	0.282895	0.282709	0.282978		0.283036	0.282990	0.282859		0.282983	0.282832	0.282739	0.282685		0.282847	0.282664		
2σ	0.000005		0.000004	0.000005	0.000004	0.000003		0.000003	0.000004	0.000010		0.000004	0.000005	0.000004	0.000004		0.000004	0.000004		

Abbreviations for rock types and groups as in Table 1.

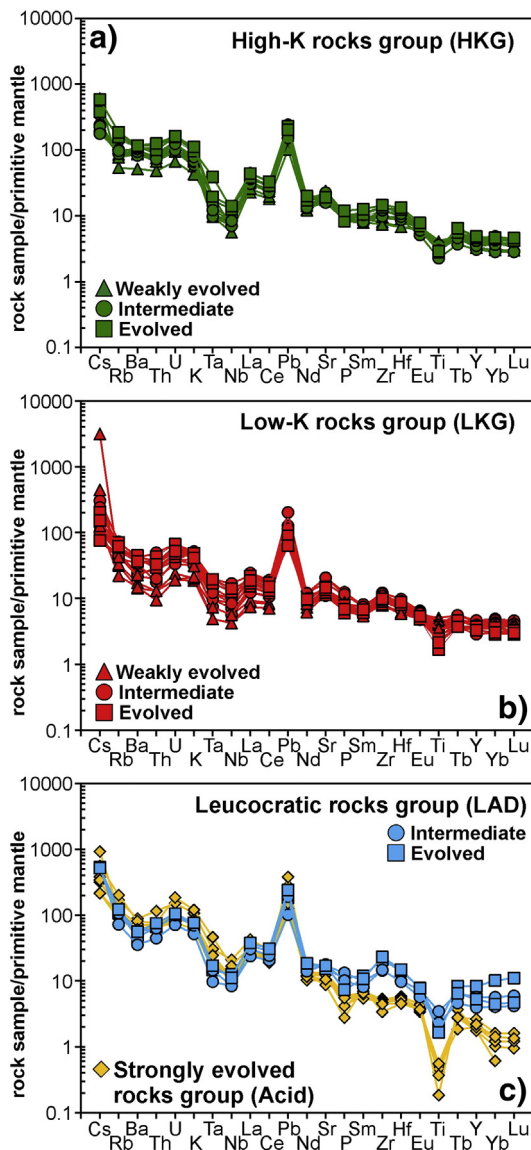


Fig. 4. Primitive mantle-normalized incompatible elements diagrams [after Sun and McDonough (1989)] for the analyzed Rodna-Bârgău igneous rocks of the a) HKG, b) LKG and c) LAD and Acid groups.

dacites), coupled with troughs at P, Zr and Ti and a strong depletion for the HREE (e.g., $La_N/Yb_N = 17.8\text{--}54.5$).

4.3. Whole rock Sr-Nd-Hf isotope data

The measured Sr-Nd-Hf isotope ratios are reported in Table 2. Rocks of the LKG group are characterized by the least radiogenic Sr ($^{87}Sr/^{86}Sr = 0.705494\text{--}0.706607$) coupled with the most radiogenic Nd ($^{143}Nd/^{144}Nd = 0.512618\text{--}0.512805$) and Hf ratios ($^{176}Hf/^{177}Hf = 0.282859\text{--}0.283036$; Fig. 5). While $^{87}Sr/^{86}Sr$ ratios do not seem to record any clear trend with increasing rock differentiation, both $^{143}Nd/^{144}Nd$ and $^{176}Hf/^{177}Hf$ show a general slight decrease moving from the least to the most evolved rock types. Similar trends characterize also the HKG rocks, although with more radiogenic Sr ($0.708039\text{--}0.709564$) and less radiogenic Nd and Hf ratios ($0.512427\text{--}0.512596$ and $0.282709\text{--}0.282895$) and with a faint increase of $^{87}Sr/^{86}Sr$ in the latest evolutionary stages. The two rock samples of the LAD group are isotopically similar to their HKG counterparts, with the andesite showing slightly lower $^{87}Sr/^{86}Sr$ coupled with higher $^{143}Nd/^{144}Nd$ and $^{176}Hf/^{177}Hf$ with respect to the dacite. Finally, a general trend of

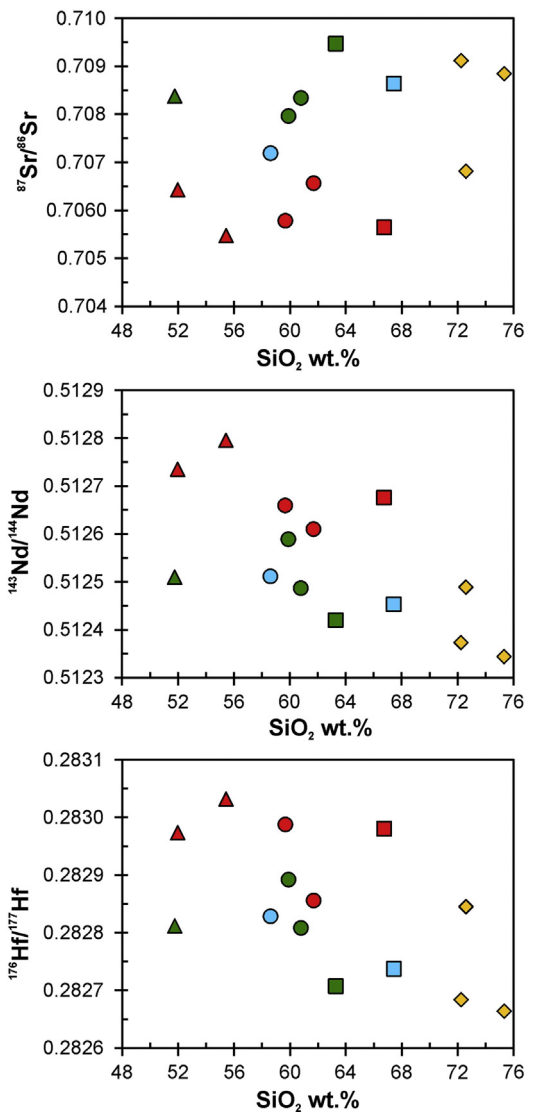


Fig. 5. $^{87}Sr/^{86}Sr$, $^{143}Nd/^{144}Nd$ and $^{176}Hf/^{177}Hf$ vs. SiO_2 plots for the analyzed Rodna-Bârgău igneous rocks. Symbols as in Fig. 2.

increasing $^{87}Sr/^{86}Sr$ and decreasing $^{143}Nd/^{144}Nd$ and $^{176}Hf/^{177}Hf$ with increasing degree of rock differentiation can be seen also in the Acid group rocks, with values covering similar spectra with respect to those observed for the rocks of the HKG.

4.4. U-Pb geochronology

The results of U-Pb zircon dating on the selected Rodna-Bârgău samples are presented in the Electronic Supplementary Material 1 (Table 8ESM). Concordia plots show that most of the data are concordant, although some inherited grains and discordant data were also recognized (Fig. 6). The latter two were obviously not taken into account in the calculation of weighted average ages. Given that precise determinations of zircon $^{207}Pb/^{235}U$ and $^{207}Pb/^{206}Pb$ are feasible usually only for Precambrian zircons (due largely to the fact that ^{235}U now comprises less than 1% of natural U and thus relatively little ^{207}Pb can be produced in the Phanerozoic), $^{206}Pb/^{238}U$ ages are here taken to indicate the crystallization ages of young zircons (see Chiu et al., 2009).

As for the LKG, both andesite and dacite samples were analyzed. In the PI-A FLN83 sample, only seven zircons were analyzed and five of them reflect an inherited population of Neoproterozoic (696 and 609 Ma), Early Cambrian (536 Ma), Early Silurian (435 Ma) and

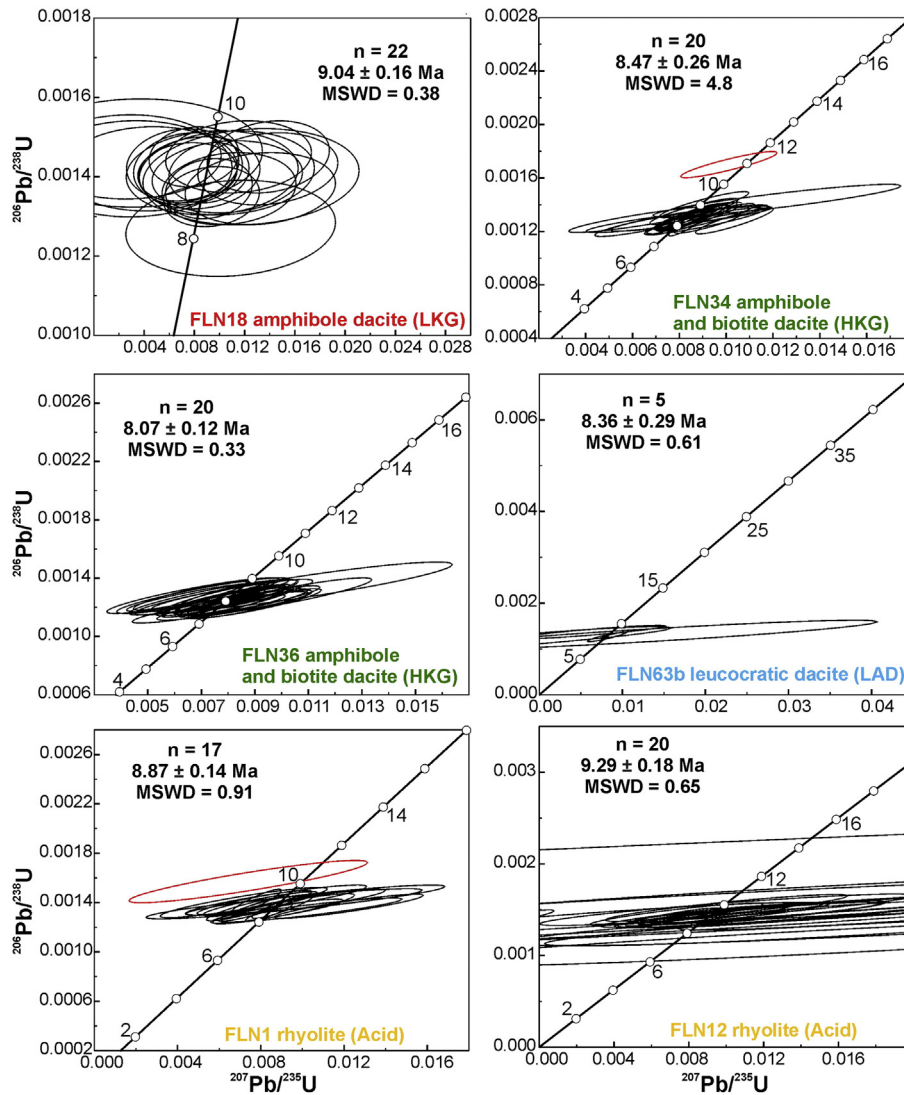


Fig. 6. Zircon U-Pb concordia diagrams for the analyzed Rodna-Bărgău igneous rocks. Data for inherited zircon populations are not shown. Error ellipses of concordant ages are 2σ . Red ellipses are for discarded non concordant data. White dots with numbers indicate ages in Ma. HKG = high-K group; LKG = low-K group; LAD = leucocratic andesite and dacite group; Acid = acid rocks group.

Cretaceous (118 Ma) age. The latter age likely reflects some Pb loss, given that in the Rodna-Bărgău area the metamorphic basement is Proterozoic to Paleozoic in age and is covered by Mesozoic to Paleogene sediments (e.g., Mason et al., 1996; Nițoi et al., 2002). The remaining two data yielded weighted mean $^{206}\text{Pb}/^{238}\text{U}$ ages of 8.1 ± 0.5 and 8.2 ± 0.6 Ma (concordia plot was therefore not shown in Fig. 6). The amphibole dacite FLN18 sample revealed two inherited Late Triassic crystals (again suggestive of some Pb loss), with the remaining 22 concordant data yielding a weighted mean $^{206}\text{Pb}/^{238}\text{U}$ age of 9.04 ± 0.16 Ma (95% confidence, MSWD = 0.38). A similar dacite sample from a close locality has been dated at 9.5 ± 0.4 Ma using the K-Ar method by Pécskay et al. (2009).

Two HKG dacites were analyzed. In sample FLN34, three inherited zircon crystals of Devonian, Jurassic and Paleocene ages (the latter two likely resulting from older crystals that experienced Pb loss during a subsequent thermal event, as for the previous samples) were found on a total of 24 analyzed spots. A single discordant 10.9 Ma age was excluded, with the remaining data yielding a weighted mean $^{206}\text{Pb}/^{238}\text{U}$ age of 8.47 ± 0.26 Ma (95% confidence, MSWD = 4.8). In sample FLN36 all the 24 spots analyzed revealed concordant ages, with a weighted mean $^{206}\text{Pb}/^{238}\text{U}$ age of 8.07 ± 0.12 Ma (95% confidence,

MSWD = 0.33). This is strongly consistent with the K-Ar age of 8.0 ± 0.3 Ma reported by Pécskay et al. (2009) for a dacite sample from the same location.

Only one sample (leucocratic dacite FLN63b) was analyzed for LAD group. Over a total of seven zircon analyzed, two indicate an inherited origin (Jurassic-Cretaceous ages of 171 and 138 Ma) and Pb loss. The remaining five concordant data yield a weighted mean $^{206}\text{Pb}/^{238}\text{U}$ age of 8.36 ± 0.29 Ma (95% confidence, MSWD = 0.61).

Two Acid group rocks have been investigated for U-Pb geochronology. In FLN1 rhyolite over 24 zircons, six reflected inherited origin (Cambrian to Cretaceous ages). As for the previous samples, the five Mesozoic ages are very likely reflecting some Pb loss, as also suggested by the lack of any correspondence between $^{206}\text{Pb}/^{238}\text{U}$ and $^{207}\text{Pb}/^{235}\text{U}$ apparent ages. After excluding a discordant 10.1 Ma age, the remaining data yielded a weighted mean $^{206}\text{Pb}/^{238}\text{U}$ age of 8.87 ± 0.14 Ma (95% confidence, MSWD = 0.91). Twenty-four zircon spots were analyzed also in FLN12 rhyolite, revealing an inherited population of four crystals ranging in age from Cretaceous to Eocene (i.e., 145.0, 71.7, 49.9 and 43.2 Ma), which also experienced Pb loss. Concordant data (20 spots) yielded a weighted mean $^{206}\text{Pb}/^{238}\text{U}$ age of 9.29 ± 0.18 Ma (95% confidence, MSWD = 0.65).

5. Discussion

The detailed sampling undertaken during this study has evidenced that the relatively small Rodna-Bârgău area hosts a large variety of rock types, possibly suggesting that numerous petrogenetic processes have occurred during a quite short time period (~3.5 Myr; Pécskay et al., 2009; this study). Although the narrow areal extension of the district (about 70 × 55 km) and the overall petrochemical similarity of the observed rock groups argue for a basically common origin, some peculiar features claim for additional petrogenetic differences. Moreover, as magmas pass through ~30–40 km of lithosphere (e.g., Dérova et al., 2006; Tari et al., 1999), it is likely that complex open-system evolutionary processes (e.g., assimilation, mixing, recharge) were also active, testified by the common occurrence of enclaves, some major scattering of the geochemical data and by the wide range of mineral phase composition and zoning patterns. This obviously makes the recognition of such processes particularly hard (as their effects are likely overlapping) and their quantitative treatment largely biased. The definition of a detailed petrogenetic model is further complicated by the overall similarity between the typical “subduction-related” geochemical signature of the Rodna-Bârgău magmatic rocks and that of the local crust and sediments, with the latter also displaying a largely variable Sr-Nd-Pb isotopic signature (see Mason et al., 1996).

In the following sections, an attempt to unravel such processes is proposed for each of the recognized rock groups, finally accounting also for their chronological and geographical distribution within the district.

5.1. The low- and high-K groups (LKG and HKG)

The great majority of the Rodna-Bârgău magmatic rocks belong to the LKG and HKG groups, as also indicated by Papp et al. (2005), who originally recognized the existence of *medium-K* and *high-K* series. Numerous are the similarities between the HKG and LKG rocks, including petrographic (largely comparable parageneses), mineral chemical

and whole rock geochemical characteristics (overlapping ranges and differentiation trends for many major and trace elements, similar incompatible elements signature). Notwithstanding this, when rocks of the same degree of evolution are compared, some differences emerge. In synthesis, when compared with LKG, the HKG rocks show 1) higher amphibole and (less evident) higher alkali feldspar contents; 2) presence of biotite, lacking in LKG rocks; 3) K₂O-richer amphibole and (less markedly) K₂O-richer feldspars; 4) stronger incompatible element enrichment (including K₂O, Ba, Rb); 5) higher ⁸⁷Sr/⁸⁶Sr plus lower ¹⁴³Nd/¹⁴⁴Nd and ¹⁷⁶Hf/¹⁷⁷Hf ratios.

It follows that the two rock groups can be considered as two different rock series. The overall linear differentiation trends displayed by both HKG and LKG (Fig. 3) suggest that both have evolved mainly through fractional crystallization, with fractionating assemblage mainly consisting of the observed mineral phases, mostly amphibole and plagioclase, with additional clinopyroxene in the earliest stages and alkali feldspar in the late stages. The main differences in the fractionating assemblage are clearly reflected by the trends of the Sr/Ba ratio with increasing differentiation (Fig. 7). Rocks of the LKG show an overall decrease of the Sr/Ba ratio, from 1.60–2.41 in the least evolved, to 0.82–2.14 in the intermediate and to 0.63–1.25 in the most evolved rocks. On the other hand, HKG rocks display much more homogeneous and basically constant values throughout (0.48–0.81), with the exception of just one amphibole microgabbro sample with Sr/Ba = 1.39, possibly caused by plagioclase accumulation. This reflects the essential role played by plagioclase fractionation in the LKG (which strongly affected the contents of compatible Sr), counterbalanced by amphibole fractionation (with respect to which Sr is incompatible) in HKG rocks. Accessory zircon is likely to have played some role in the late stages of magma evolution of the LKG, as evidenced by the decrease of Pb, Zr, Y and HREE. Additional processes other than fractionation are testified by some scattering of major- and trace element variation trends, as well as by large compositional variations of some of the analyzed mineral phases. In addition, since each subvolcanic body is homogeneous from a petrographic point of view, it might have experienced an

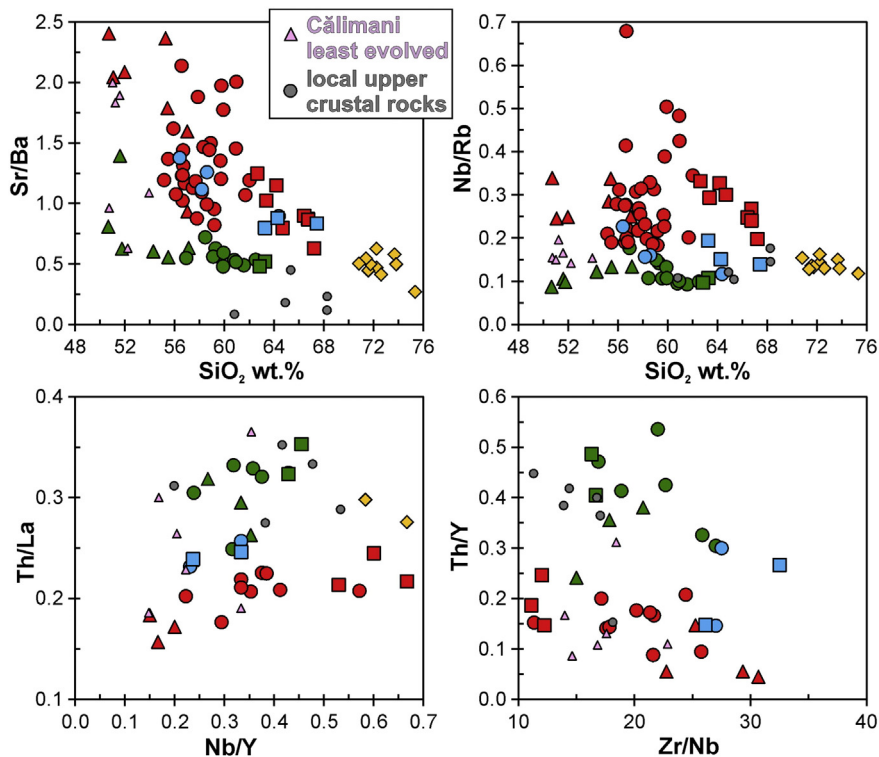


Fig. 7. Binary plots of inter-element ratios for the analyzed Rodna-Bârgău igneous rocks. Symbols as in Fig. 2. Data for the least evolved rocks from the Călimani district (MgO > 4 wt.%) and for the local upper crustal rocks are from Mason et al. (1996).

independent differentiation history (giving rise to several independent liquid lines of descent) and a variably complex open-system evolution.

The definition of HKG and LKG source composition appears quite difficult to be addressed, as the least evolved rocks of both series are clearly not primitive (as indicated by the relatively low Mg#, Ni and Cr and the lack of forsteritic olivine). Incompatible element ratios such as Nb/Y (0.27–0.35 for HKG, 0.15–0.24 for LKG), Th/Y (0.24–0.36 and 0.04–0.15) and La/Nb (2.60–4.48 and 1.60–2.63), fall in the ranges for the least evolved products (MgO >4 wt.%) from the neighboring Călimani volcanic district, few km to the southeast (e.g., Nb/Y = 0.15–0.33, Th/Y = 0.09–0.31, La/Nb = 1.71–4.00; Mason et al., 1996; Fig. 7). Such similarity can be observed also for isotope ratios and extends also to the other districts of the East Carpathians, basically defining a mixing trajectory between a high- ϵ_{Nd} source (DMM- Depleted MORB Mantle - for Călimani, Gurghiu and Northern Harghita, EAR - European Asthenospheric Reservoir - for Southern Harghita) and a high- ϵ_{Sr} subducted terrigenous sediments component (represented by local flysch deposits; Fig. 8). A metasomatically-modified mantle source can be thus proposed also for the Rodna-Bărgău HKG and LKG rocks, with differences in isotope ratios reflecting a higher sedimentary input for the first. Assuming a slightly higher sediment contribution in the genesis of the HKG parental magmas would also explain: 1) the higher H₂O content reflected by the higher amphibole stability (mainly at the expenses of the plagioclase stability field which, conversely, is the dominant mineral phase in the LKG magmas); 2) the overall higher enrichment of LILE and LREE; 3) the higher values of inter-element ratios indicative of an enrichment in fluid-mobile elements such as Th/Y, Ba/Zr (3.99–7.27 vs. 1.12–1.56 of LKG counterparts) Th/La (0.26–0.32 vs. 0.16–0.24), Th/Yb (2.16–3.80 vs. 0.40–1.39) and Th/Nb (0.68–1.43 vs. 0.27–0.63).

Alternatively, it could be proposed that the HKG geochemical features were acquired by open system-processes involving LKG magmas and local crustal rocks. It should be however noted that during the evolution of HKG magmas, both the isotopic ratios and many incompatible element ratios did not substantially change or only slightly increased (Fig. 7). As mineralogical and petrochemical evidence indicate that HKG magmas did interact with crustal rocks, it appears that such interaction did not substantially modify these features. This is confirmed by the few upper crustal basement rock compositions reported by Mason et al. (1996) for the Călimani district, showing similar Th/La (0.28–0.49), Th/Y (0.15–0.45), Nb/Y (0.20–0.60) and Nb/Rb (0.10–0.18) with respect to HKG rocks. As a consequence, the geochemical characteristics of HKG primary magmas are unlikely to

be the product of a LKG magma-crust interaction, as this would require an unrealistically high mass of contaminant. This is confirmed by the results of the AFC models displayed in Fig. 9. To account for the wide compositional range of local upper crustal rocks, both the least Sr radiogenic and the most Sr radiogenic compositions from the existing literature were considered. The only models that reproduces the transition from the least evolved LKG magma to those of the HKG series are those assuming a contaminant with extremely high $^{87}Sr/^{86}Sr$ (0.73619) and a D_{Sr} of 0.1 and 0.5. However, in the first case, the model requires a rate of assimilation/rate of crystallization r of ~0.5, whereas in the second requires r ~ 0.3 and a quite low value of the residual melt fraction (f ~ 0.5–0.6). Therefore, both models can be discarded.

While the evolution of HKG rock series seems to have occurred mainly in the upper crust, the evolution of LKG magmas seem to have been more complex. This is particularly evident for the intermediate rocks of this series, as they are clearly those with the largest spread in composition for mineral phases (e.g., An_{45–89}Ab_{10–54}Or_{0–2} for plagioclase), major- and trace elements (e.g., K₂O = 0.50–1.55 wt.%, Na₂O = 2.69–3.85 wt.%, Ba = 133–318 ppm, Nb = 5–26 ppm) and inter-element ratios (e.g., Sr/Ba = 0.88–2.14, Nb/Rb = 0.18–0.68, Nb/Y = 0.22–0.57, Zr/Nb = 11.3–25.8). On the other hand, both the least evolved and the evolved rocks of the LKG generally display a more homogeneous compositional spectra. It thus appears likely that least evolved LKG magmas experienced significant open system differentiation during their evolution to intermediate compositions.

As for the possible contaminant material for the rocks of the LKG series, a major involvement of the local upper crust can be ruled out since this has very low Nb/Rb, high Th/La and high Th/Y (Mason et al., 1996), while the least evolved to intermediate LKG magmas are characterized by high and variable Nb/Rb (0.14–0.35) and substantially constant low Th/La (0.16–0.25) and low Th/Y (0.06–0.20). On the other hand, an interaction with lower crustal rocks cannot be excluded, considering that global estimates for such lithologies (Rudnick and Gao, 2003) have higher Nb/Rb (~0.45), lower Th/La (~0.15) and lower Th/Y (~0.08). A direct test with local lower crust cannot be made, because the only lower crustal (granulite) xenoliths available in literature are from the Pannonian Basin (Dobosi et al., 2003; Embey-Isztin et al., 2003), belonging to the AlCaPa plate. However, interaction of LKG magmas with the Proterozoic-Paleozoic basement is testified by the common occurrence of metamorphic enclaves (see ESM2), as well as by inherited zircon crystals of consistent ages. Other xenocrystic material of possibly deep provenance include the ^{VI}Al-rich, Mg- and Ca-poorer amphiboles observed in LKG dacites, as suggested by their Al# > 0.21 (Al# = ^{VI}Al/Al_{tot}), typical of high-P amphiboles (Ridolfi et al., 2010). The almandine garnet occasionally occurring in some LKG andesites and dacites might have a similar xenocrystic origin, as also suggested by Nițoi et al. (2002). However, it should be noted that garnet crystals with comparable composition (Sps 4–10, Grs 6–18) found within Middle Miocene andesitic to dacitic rocks from the northern Pannonian Basin (West Carpathians) were considered as a high-pressure primary crystallizing phase by Harangi et al. (2001). Therefore, an alternative hypothesis for the garnet crystals recovered in the LKG andesites and dacites could involve a direct segregation from a melt that was enriched in Al₂O₃ due to the interaction with metasedimentary crustal lithologies, as suggested by the slightly to markedly peraluminous character of the LKG dacites (A/CNK = 0.96–1.29). Whatever their origin, the occurrence of these garnets argues in favor of a lower crustal involvement. In addition, their common preservation as unreacted crystals in LKG dacites can be taken as an evidence for a rapid magma ascent, consistent with the homogeneous composition of LKG dacites that indicates negligible interaction with wall rock.

5.2. The acid and leucocratic (LAD) groups

The rocks of the Acid and LAD groups crop out as very small occurrences and in opposite peripheral areas of the Rodna-Bărgău district

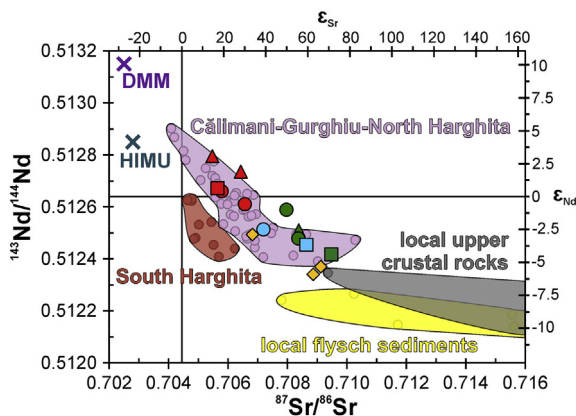


Fig. 8. $^{143}Nd/^{144}Nd$ vs. $^{87}Sr/^{86}Sr$ plot for the analyzed Rodna-Bărgău igneous rocks. Symbols as in Fig. 2. The fields for the igneous rocks from the Călimani-Gurghiu-North Harghita and South Harghita East Carpathian district, as well as those for the local upper crust (extending up to $^{143}Nd/^{144}Nd = 0.512057$ and $^{87}Sr/^{86}Sr = 0.72431$) and flysch sediments (up to $^{143}Nd/^{144}Nd = 0.512126$ and $^{87}Sr/^{86}Sr = 0.72740$) are drawn after Mason et al. (1996). The depleted MORB mantle (DMM) and high- μ (HIMU), representative of the Enriched Asthenospheric Reservoir, EAR) mantle components are as defined by Zindler and Hart (1986).

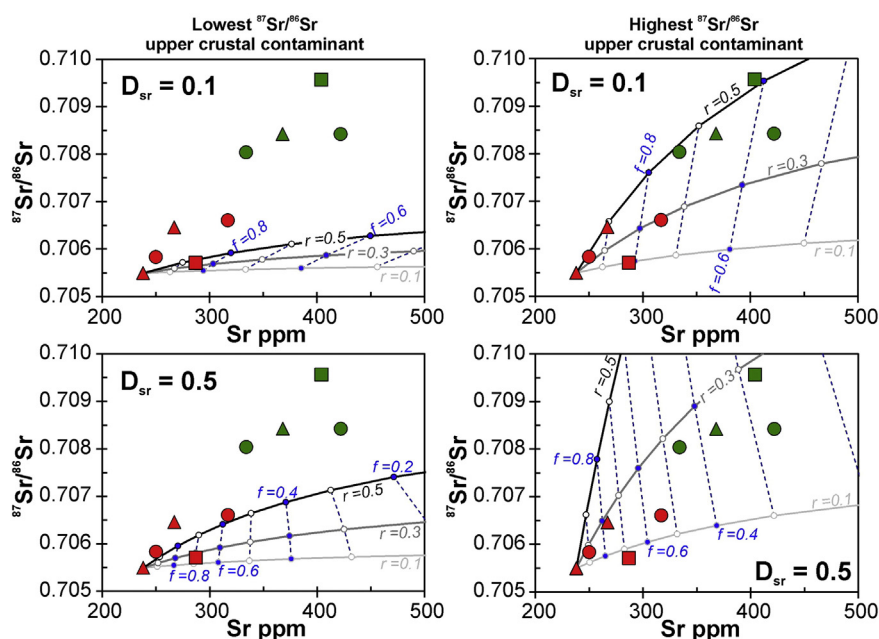


Fig. 9. Results of the AFC model (DePaolo, 1981) for the genesis of HKG least evolved rocks through interaction of LKG least evolved magmas (represented by amphibole- and clinopyroxene-basaltic andesite sample FLN79) with local upper crustal rocks (from Mason et al., 1996). Symbols as in Fig. 2. Black, dark gray and light gray lines, refer respectively to values of 0.5, 0.3 and 0.1 for the ratio $r =$ rate of assimilation/rate of crystallization. Blue dashed lines are for the residual liquid fraction f . Left column assumes a contaminant with the lowest reported $^{87}\text{Sr}/^{86}\text{Sr}$ (0.70936, sample CB3). Right column assumes a contaminant with the highest reported $^{87}\text{Sr}/^{86}\text{Sr}$ (0.73619, sample CB7). The bulk partition coefficient for Sr (D_{Sr}) was set to 0.1 and 0.5 (upper and lower row, respectively).

(Fig. 1). The strongly evolved rhyolites (including microgranites) have been considered by Papp et al. (2005) to be part of the low- K group rocks (their *medium-K series*), as indicated by the quite linear differentiation trends linking them. Notwithstanding this, there are some clues that possibly suggest an origin independent from LKG magmas. First, the large compositional gap separating LKG dacites from the Acid rocks (e.g., ~ 3.50 wt.% SiO_2) suggests that there is not continuous spectrum of magma composition between the two. Second, the transition from LKG dacites to the Acid rocks is not marked by Ba, Sr and Eu troughs in primitive mantle-normalized diagrams, as it would be instead expected after significant feldspar fractionation. Third, the Rodna-Bârgău rhyolites and microgranites have very low Fe_2O_3 , CaO and MgO and high A/CNK, contrasting with typical metaluminous to weakly peraluminous M-type granites (e.g., Chappell et al., 2012; Clemens et al., 2011). Finally, to achieve such strongly peraluminous character, fractional crystallization of metaluminous phases would be necessary. The most likely candidate for this is amphibole, which, however, does not appear to be a major fractionating phase for the low- K amphibole dacites.

The genesis of the Rodna-Bârgău Acid rocks thus requires an alternative explanation, involving either interaction of LKG dacites with Al-rich crustal rocks or partial melting of igneous or sedimentary crustal rocks. The first appears a viable hypothesis, as the local upper crust has been demonstrated to include peraluminous metapelitic schists and gneisses (e.g., Mason et al., 1996), but would require simultaneous fractionation of garnet or zircon to produce the observed marked depletion in HREE (Fig. 4). Although some zircon crystals were actually recognized in the Rodna-Bârgău Acid rocks, their abundance appears to be too low to produce such strong effect. An origin via partial melting of an Al-rich source appears therefore more likely. This is also consistent with the mafic mineral-poor composition and feldspar-quartz-dominated paragenesis of the Acid rocks, suggesting a composition close to granite minimum.

According to Chappell (1999), Chappell and White (2001) and Clemens and Stevens (2012), a geochemical distinction between I- and S-type granites is extremely hard for rocks with very high SiO_2 like the Rodna-Bârgău Acid rocks. However, the relatively high Na_2O , CaO/FeO (1.47–2.15) and Sr, the quite regular element variations

(e.g., Fig. 3) and the linear decrease of P_2O_5 with increasing SiO_2 observed for the Rodna-Bârgău rhyolites and microgranites, seem more consistent with an igneous source. This is also suggested by their very low Rb/Ba (0.14–0.17, except for the silica-richer FLN2 having 0.23) and Rb/Sr (0.21–0.38, FLN2 = 0.70) and relatively high CaO/ Na_2O (0.47–0.73), values which, according to Sylvester (1998), are indicative of a plagioclase-rich and clay-poor source. An I-type origin apparently contrasts with their strongly peraluminous character, a feature that is typically ascribed to S-type granites. However, as illustrated by Kamei (2002) and by the experimental results from Beard and Lofgren (1991), melting of a metaluminous basic to intermediate source at lower to middle crustal depths can generate I-type peraluminous melts. These authors demonstrated that water-saturated melting can produce strongly peraluminous LILE-enriched and HFSE-depleted melts (with higher A/CNK at lower degrees of melting), in equilibrium with an amphibole-rich residue. The relatively low $^{87}\text{Sr}/^{86}\text{Sr}$ and high $^{143}\text{Nd}/^{144}\text{Nd}$ and $^{176}\text{Hf}/^{177}\text{Hf}$ values (especially for rhyolite FLN12), similar to those of HKG rocks, is also consistent with an I-type origin. As Acid rocks are characterized by increasing $^{87}\text{Sr}/^{86}\text{Sr}$, coupled with decreasing $^{143}\text{Nd}/^{144}\text{Nd}$ and $^{176}\text{Hf}/^{177}\text{Hf}$ with increasing differentiation, it could be speculated that the crustal melts had variably ponded within and interacted with crustal rocks.

As for the leucocratic rock group, which occurrence in the Rodna-Bârgău area is here reported for the first time, their unusual petrographic and petrochemical features suggest that their genesis involved a relatively H_2O -poor parental magma, which appears difficult to be linked with those of the hydrous HKG and LKG series. Given that no near-primitive basic rock has been found to belong to the LAD group, an origin via decompression melting of some crustal mafic rocks close to Moho depths (as their relatively high Y and HREE contents are consistent with a process leaving no garnet in the residue) might be considered. In this instance, the linear trends linking the leucocratic andesites and dacites could be due to differentiation processes.

In order to test the crustal anatexic origin for both the Acid and the leucocratic rock groups, a simplified model of equilibrium (due to the intrinsic complexity of modeling disequilibrium melting; e.g., McLeod et al., 2012) modal batch melting (to avoid complications resulting

from uncertainties on incongruent melting reactions) has been carried out. Given the lack of literature data for the basic (possibly amphibolitic) rocks of the local metamorphic basement, the least evolved HKG and LKG rocks were used as representative for the composition of the potential source material. Amphibole-rich and amphibole-poor residues were assumed, respectively for Acid and LAD group rocks, following the model of Borg and Clynne (1998). According to these authors, melting of a lower crustal amphibolitic source at variable $f(\text{H}_2\text{O})$ conditions (influencing the plagioclase/amphibole ratio in the source) can produce both SiO_2 - and H_2O -rich and SiO_2 - and H_2O -poor felsic magmas similar to the Rodna-Bârgău rhyolites and leucocratic andesites, respectively. The first, characterized by a ferromagnesian assemblage dominated by amphibole and biotite, are generated at relatively high $P(\text{H}_2\text{O})$ and relatively low T (~2 kbar and ~900 °C). The second, with orthopyroxene (\pm clinopyroxene) as the main ferromagnesian mineral, require $P(\text{H}_2\text{O})$ ~1 kbar and T ~950 °C. The primitive mantle-normalized incompatible element patterns of the Rodna-Bârgău Acid rocks can be reproduced with “hydrous” melting models only if the presence of additional residual garnet and zircon (respectively lowering the abundances of Y-HREE and Zr-Hf) is assumed (Fig. 10). A less enriched LKG-like source seems more likely, as it requires lower degrees of melting ($F \leq 5\%$) compared to a more enriched HKG-like one ($F \sim 30\%$). On the other hand, although the global pattern displayed by LAD rocks is quite adequately reproduced by the “anhydrous” melting model (Fig. 11), the resulting melts are too poor in Sr and require high degrees of partial melting ($F \sim 30$ and $\sim 50\%$ using LKG- and HKG-like source compositions, respectively). Both the inconsistencies can be overcome assuming that the actual source rock is represented by a more primitive, less enriched

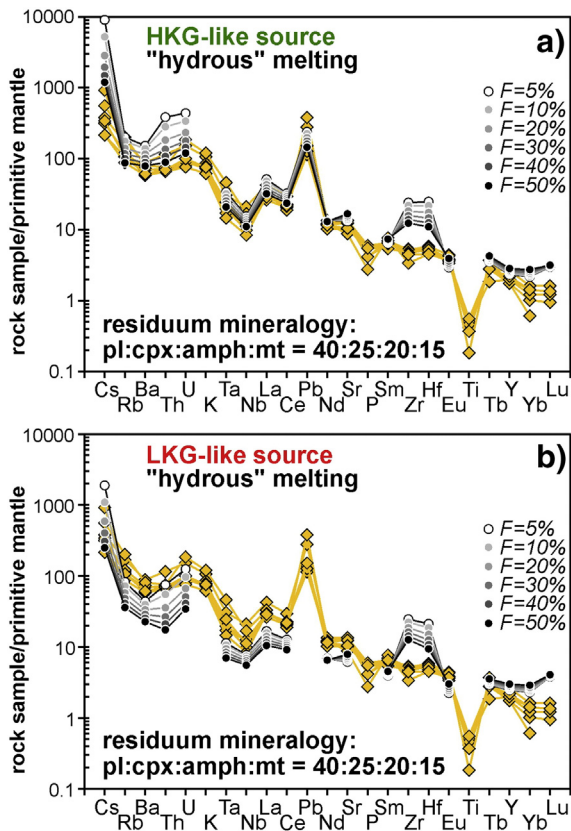


Fig. 10. Results of modal batch melting model for the genesis of the Rodna-Bârgău Acid rocks assuming “hydrous” melting of a) LKG-like (sample FLN79) and b) HKG-like (sample FLN22) source at various degrees of partial melting F (dots color getting darker with values increasing from 5 to 50%). Modes of the source residuum are from Borg and Clynne (1998). Mineral/melt partition coefficients were taken from Nash and Crecraft (1985), Bacon and Druitt (1988), Sisson and Bacon (1992), Ewart and Griffin (1994), Sisson (1994).

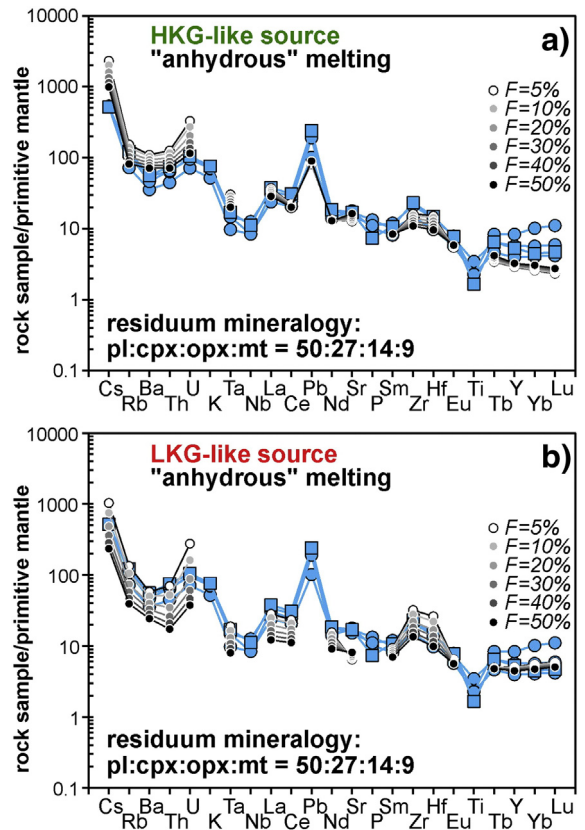


Fig. 11. Results of modal batch melting model for the genesis of the Rodna-Bârgău leucocratic rocks assuming “anhydrous” melting of a) LKG-like (sample FLN79) and b) HKG-like (sample FLN22) source at various degrees of partial melting F (dots color getting darker with values increasing from 5 to 50%). Modes of the source residuum are from Borg and Clynne (1998). Mineral/melt partition coefficients were taken from Luhr and Carmichael (1980), Bacon and Druitt (1988), Ewart and Griffin (1994), Sisson (1994), Brennan et al. (1995).

basic rock having lesser modal plagioclase, which is also more likely to be practically amphibole-free.

5.3. The spatial and chronological evolution of Rodna-Bârgău magmatism

The notable variety of lithotypes observed in the Rodna-Bârgău subvolcanic district claims for a complex petrogenetic history, which was also influenced by the local geological context, as rock compositions are related with geographic location (Fig. 1). While intermediate “andesitic” rocks crop out extensively, weakly evolved rocks are found in a limited area depicting a fine NW-SE array in the central-southern sector. Evolved “dacitic” rocks are found in few outcrops of the northern and eastern sectors and strongly evolved Acid rocks crop out only in a very narrow area in the northwestern-most tip of the district. In addition, HKG and LKG rocks appear to be separated by a NW-SE lineament, suggesting a notable structural control that is also consistent with the orientation of the extensional axes related with the 12–10 Ma transensional stage (Gröger et al., 2008; Tischler et al., 2007, 2008).

On the other hand, estimated ages do not seem to follow a very precise chronological scheme. Although Papp et al. (2005) proposed that low-K rocks are older than the high-K ones (~10.6 vs. ~9 Ma), the geochronological data reported by Pécskay et al. (2009) argue against this. About 25 K-Ar ages on whole rock samples (plus some on separated phenocrysts or groundmass) allowed these authors to identify an overall time interval of 11.5–8 Ma, with no relationship between estimated ages and rock compositions, except for the rhyolites being emplaced only during the latest stages (i.e., ~8 Ma). The U-Pb zircon ages presented here (from 9.29 to 8.07 Ma) fall well within such age

range and perfectly match literature data when samples from broadly the same location are taken into account. In addition, the 8.87 and 9.29 Ma ages obtained for rhyolite samples indicate that there is substantially no precise link between rock types and emplacement ages, although the strongly evolved rocks still seem to have not characterized the earliest magmatic stages in the district.

Based on the above evidences, it can be proposed that the contemporaneous emplacement of both HKG and LKG rocks in two distinct sectors of the Rodna-Bârgău area reflects the involvement of two contiguous mantle domains showing very slight differences. Melting of such mantle sources was likely related to the Early-Middle Miocene post-collisional extension (17–14 Ma; e.g., Seghedi et al., 2004), although magma upwelling and emplacement was strongly obstructed by the local 16–12 Ma transpressional tectonic stage. This possibly resulted in a significant magma/crust interaction, witnessed by the abundant xenoliths/xenocrysts and by the mineralogical and petrochemical evidences for a substantial open system evolution presented above. While HKG rocks seem to have evolved mainly within the upper crust, the differentiation history of LKG rocks likely occurred at deeper levels, possibly involving significant interaction with lower crustal rocks. This is particularly true for the intermediate LKS andesites, possibly because upwelling magmas had met the conditions for stagnation due to the presence of a density trap represented by the local thick lithosphere. When magmas finally reached an evolved dacitic composition, their density was sufficient to allow their ascent and prevent further substantial contamination. Therefore, it could be speculated that the two neighboring areas in which HKG and LKG rocks occur are also characterized by different crustal conditions (in terms of thickness and/or composition), variably influencing the ascent of magmas.

When the local tectonic regime switched to transtensional around 12–10 Ma, HKG and LKG magmas more easily found their way to the upper levels and possibly supplied sufficient thermal surplus to trigger crustal melting processes of amphibolitic lithologies that generated the rocks of the Acid group. The precisely localized occurrence of such rocks is likely related to the presence of particularly favorable conditions, which apparently did not characterize any other sector of the district. On the other hand, the crustal anatexis origin proposed for the rocks of the LAD group needs to be related to a substantially different process. Their H₂O-poor paragenesis argues for a substantially anhydrous source that requires a significant thermal pulse to undergo partial melting. Given the very young age estimate of 8.36 Ma obtained for one sample from this group, it could be suggested that crustal melting was also related to the progressive SE-shifting of the East Carpathian magmatism to the Călimani district, which experienced its climax activity during the 10–8 Ma period (Seghedi et al., 2005).

6. Conclusions

Besides the typical “subduction-related” geochemical signature, magmatism in the Late Miocene Rodna-Bârgău district shows several features that could be connected to its post-collisional setting: (a) absence of primitive lithotypes, (b) relatively narrow magma evolution from (basaltic) andesite to dacite, (c) variable, small volume, complex open-system evolution, implying interaction with lower and upper crustal material, (d) evidences for large shallow subcontinental mantle heterogeneities, (e) small volume, younger, rocks generated via crustal anatexis from decompression melting and increased heat from the neighboring mantle melting, occurring in opposite peripheral areas.

Magmatism was deeply influenced by tectonics, both at the global and at the local scale. The complex geodynamic evolution of the East Carpathians area had likely provided the conditions for the juxtaposition of different mantle domains in the Rodna-Bârgău area, which lies close to the intersecting point between the East European, Tisza-Dacia and AlCaPa plates. Melting of such sources, probably related to the early 17–14 Ma post-collisional crustal extension, produced the calcalkaline magmas of the predominant HKG and LKG groups, cropping

out in two distinct central sectors of the district, separated by an evident NW-SE tectonic lineament. The HKG rocks, with higher amphibole abundances, incompatible elements contents, ⁸⁷Sr/⁸⁶Sr ratios and lower ¹⁴³Nd/¹⁴⁴Nd and ¹⁷⁶Hf/¹⁷⁷Hf, were likely generated from a metasomatically-enriched mantle source with a stronger input of the terrigenous sedimentary metasomatic component with respect to the amphibole-poorer and plagioclase-richer LKG rocks.

The 16–12 Ma local transpressional tectonic regime did not allow significant upwelling of the produced magmas, which thus underwent significant interaction with crustal lithologies, as witnessed by numerous petrographic, mineralogical, and geochemical evidences (e.g., xenoliths, mineral disequilibria, variability of isotope and interelement ratios, inherited zircon populations etc.). Magmas of the HKG interacted mainly with upper crustal rocks, whereas LKG magmas experienced a deep interaction with lower crustal rocks, mostly during the evolution to andesitic compositions.

The transition to a 12–10 Ma transtensional regime not only favored magma uprising, but also allowed hydrous decompression partial melting of the amphibolitic basement rocks in the westernmost sector of the Rodna-Bârgău district, giving rise to the peraluminous strongly evolved magmas of the Acid group. Finally, the southeastward shifting of the magmatism to the Călimani volcanic district furnished surplus heat to allow anhydrous partial melting of relatively amphibole-free metabasic lithologies and generate the leucocratic hydrous-poor magmas of the LAD group, occurring only in the southern-easternmost sector of the area.

Acknowledgements

The authors wish to thank Dr. Mihai Tatu, Răzvan-Gabriel Popa and Gheorghe Pârnu, Giuliana Buongiovanni, Roberto de' Gennaro and Chiu-Hung Chu, Hao-Yang Lee and Jui-Ting Tang for assistance respectively during field activities, sample preparation, EDS microanalyses and isotope analyses. The comments from two anonymous reviewers and the Editor Andrew Kerr greatly contributed to improve the quality and the clearness of the manuscript. Financial support was provided by “Programma di Mobilità POR Campania FSE 2009–2013” (to L.F. and F.L.), Ricerca Dipartimentale (to L.F. and V.M.), PRIN 2010–2011 20107ESMX9_001 (to V.M., Principal Investigator Prof. L. Melluso) and CNCS-UEFISCDI, project number PN-II-IDPCE-2012-4-0137 (from the Ministry of Education and Scientific Research, to I.S.) grants. ML acknowledges La Sapienza grants (*Ricerche Ateneo* 2014 and 2015).

Appendix A. Supplementary data

Supplementary data to this article can be found online at doi:10.1016/j.lithos.2016.10.015.

References

- Andersen, T., 2002. Correction of common lead in U-Pb analyses that do not report ²⁰⁴Pb. *Chemical Geology* 192, 59–79.
- Arculus, R.J., 2003. Use and abuse of the terms calcalkaline and calcalkalic. *Journal of Petrology* 44, 929–935.
- Bacon, C.R., Druitt, T.H., 1988. Compositional evolution of the zoned calcalkaline magma chamber of Mt. Mazama, crater Lake, Oregon. *Contributions to Mineralogy and Petrology* 98, 224–256.
- Beard, J.S., Lofgren, G.E., 1991. Dehydration melting and water-saturated melting of basaltic and andesitic greenstones and amphibolites at 1, 3 and 6.9 kb. *Journal of Petrology* 32, 365–401.
- Borg, L.E., Clyne, M.A., 1998. The petrogenesis of felsic calc-alkaline magmas from the southernmost Cascades, California: origin by partial melting of basaltic lower crust. *Journal of Petrology* 39, 1197–1222.
- Brenan, J.M., Shaw, H.F., Ryerson, F.J., Phinney, D.L., 1995. Experimental determination of trace-element partitioning between pargasite and a synthetic hydrous andesitic melt. *Earth and Planetary Science Letters* 135, 1–11.
- Carminati, E., Lustrino, M., Doglioni, C., 2012. Geodynamic evolution of the central and western Mediterranean: tectonics vs. igneous petrology constraints. *Tectonophysics* 579, 173–192.
- Chappell, B.W., 1999. Aluminium saturation in I- and S-type granites and the characterization of fractionated haplogranites. *Lithos* 46, 535–551.

- Chappell, B.W., White, J.R., 2001. Two contrasting granite types: 25 years later. *Australian Journal of Earth Sciences* 48, 489–499.
- Chappell, B.W., Bryant, C.J., Wyborn, D., 2012. Peraluminous I-type granites. *Lithos* 153, 142–153.
- Chiu, H.-Y., Chung, S.-L., Wu, F.-Y., Liu, D., Liang, Y.-H., Lin, I.-J., Iizuka, Y., Xie, L.-W., Wang, Y., Chu, M.-F., 2009. Zircon U-Pb and Hf isotopic constraints from eastern Transhimalayan batholiths on the precollisional magmatic and tectonic evolution in southern Tibet. *Tectonophysics* 477, 3–19.
- Clemens, J.D., Stevens, G., 2012. What controls chemical variation in granitic magmas? *Lithos* 134–135, 317–329.
- Clemens, J.D., Stevens, G., Farina, F., 2011. The enigmatic source of I-type granites: the peritectic connection. *Lithos* 126, 174–181.
- Csontos, L., Nagymarosy, A., Horváth, F., Kovács, M., 1992. Tertiary evolution of the Intra-Carpathian area: a model. *Tectonophysics* 208, 221–241.
- DePaolo, D.J., 1981. Trace element and isotopic effects of combined wallrock assimilation and fractional crystallization. *Earth and Planetary Science Letters* 53, 189–202.
- Dérierova, J., Zeyen, H., Bielik, M., Salman, K., 2006. Application of integrated geophysical modeling for determination of the continental lithospheric thermal structure in the eastern Carpathians. *Tectonics* 25, TC3009. <http://dx.doi.org/10.1029/2005TC001883>.
- Dobosi, G., Kempton, P.D., Downes, H., Embey-Isztin, A., Thirlwall, M., Greenwood, P., 2003. Lower crustal granulite xenoliths from the Pannonian basin, Hungary, part 2: Sr-Nd-Pb-Hf and O isotope evidence for formation of continental lower crust by tectonic emplacement of oceanic crust. *Contributions to Mineralogy and Petrology* 144, 671–683.
- Embey-Isztin, A., Downes, H., Kempton, P.D., Dobosi, G., Thirlwall, M., 2003. Lower crustal granulite xenoliths from the Pannonian basin, Hungary, part 1: mineral chemistry, thermobarometry and petrology. *Contributions to Mineralogy and Petrology* 144, 652–670.
- Ewart, A., Griffin, W.L., 1994. Application of proton-microprobe data to trace-element partitioning in volcanic rocks. *Chemical Geology* 117, 251–284.
- Geological map of Romania scale 1:200000, sheets L35-I Viseu, L35-II Rădăuți, L35-VIII Bistrița, L35-VIII Toplița, 1967–1969. Geological Institute of Romania.
- Gröger, H.R., Fügenschuch, B., Tischler, M., Schmid, S.M., Foeken, P.T., 2008. Tertiary cooling and exhumation history in the Maramures area (internal eastern Carpathians, northern Romania): thermochronology and structural data. In: Siegesmund, S., Fügenschuch, B., Froitzheim, N. (Eds.), *Tectonic Aspects of the Alpine-Dinaride-Carpathian System*. Geological Society of London Special Publications Vol. 298, pp. 169–195.
- Handy, M.R., Schmid, S.M., Bousquet, R., Kissling, E., Bernoulli, D., 2010. Reconciling plate-tectonic reconstructions of Alpine Tethys with the geological-geophysical record of spreading and subduction in the Alps. *Earth-Science Reviews* 102, 121–158.
- Harangi, S., Lenkey, L., 2007. Genesis of the Neogene to Quaternary volcanism in the Carpathian-Pannonian Region: role of subduction, extension and mantle plume. In: Beccaluva, L., Bianchini, G., Wilson, M. (Eds.), *Cenozoic Volcanism in the Mediterranean Area*. Geological Society of America Special Paper Vol. 418, pp. 67–92.
- Harangi, S., Downes, H., Kósa, L., Szabó, C., Thirlwall, M.F., Mason, P.R.D., Matthey, D., 2001. Almandine garnet in calc-alkaline volcanic rocks of the northern Pannonian basin (eastern-central Europe): geochemistry, petrogenesis and geodynamic implications. *Journal of Petrology* 42, 1813–1843.
- Harangi, S., Downes, H., Seghedi, I., 2006. Tertiary-Quaternary subduction processes and related magmatism in the Alpine-Mediterranean region. In: Gee, D., Stephenson, R. (Eds.), *European Lithosphere Dynamics*. Geological Society of London Memoirs Vol. 32, pp. 167–190.
- Harangi, S., Sági, T., Seghedi, I., Ntaflou, T., 2013. A combined whole-rock and mineral-scale investigation to reveal the origin of the basaltic magmas of the Perșani monogenetic volcanic field, Romania, eastern-central Europe. *Lithos* 180–181, 43–57.
- Jurje, M., Ionescu, C., Hoecq, V., Kovacs, M., 2014. Geochemistry of Neogene quartz andesites from the Oaș and Gutâi Mountains, Eastern Carpathians (Romania): a complex magma genesis. *Mineralogy and Petrology* 108, 13–32.
- Kamei, A., 2002. Petrogenesis of Cretaceous peraluminous granite suites with low initial Sr isotopic ratios, Kyushu Island, southwestern Japan arc. *Gondwana Research* 5, 813–822.
- Kiss, B., Harangi, S., Ntaflou, T., Mason, P.R.D., Pál-Molnár, E., 2014. Amphibole perspective to unravel pre-eruptive processes and conditions in volcanic plumbing systems beneath intermediate arc volcanoes: a case study from Ciomadul volcano (SE Carpathians). *Contributions to Mineralogy and Petrology* 167:986. <http://dx.doi.org/10.1007/s00410-014-0986-6>.
- Kręzek, C., Bally, A.W., 2006. The Transylvanian Basin (Romania) and its relation to the Carpathian fold and thrust belt: insights in gravitational salt tectonics. *Marine and Petroleum Geology* 23, 405–442.
- Le Maitre, R.W., 2005. *Igneous rocks. A classification and glossary of terms. Recommendations of the International Union of Geological Sciences Subcommittee on the Systematics of Igneous Rocks*, Second edition Cambridge University Press, Cambridge (236 pp.).
- Lee, H.-Y., Chung, S.-L., Ji, J., Qian, Q., Galley, S., Lo, C.-H., Lee, T.-Y., Zhang, Q., 2012. Geochemical and Sr-Nd isotopic constraints on the genesis of the Cenozoic Linzizong volcanic successions, southern Tibet. *Journal of Asian Earth Sciences* 53, 96–114.
- Luhr, J.F., Carmichael, I.S.E., 1980. The Colima volcanic complex, Mexico I. Post-caldera andesites from Volcan Colima. *Contributions to Mineralogy and Petrology* 71, 343–372.
- Lukács, R., Harangi, S., Bachmann, O., Guillong, M., Danišik, M., Buret, Y., von Quadt, A., Dunkl, I., Fodor, L., Sliwinski, J., Soós, I., Szepesi, J., 2015. Zircon geochronology and geochemistry to constrain the youngest eruption events and magma evolution of the Mid-Miocene ignimbrite flare-up in the Pannonian Basin, eastern central Europe. *Contributions to Mineralogy and Petrology* 170:52. <http://dx.doi.org/10.1007/s00410-015-1206-8>.
- Lustrino, M., Duggen, S., Rosenberg, C., 2011. The central-western Mediterranean: anomalous igneous activity in an anomalous collisional tectonic setting. *Earth-Science Reviews* 104, 1–40.
- Mason, P.R.D., Downes, H., Seghedi, I., Szakács, A., Thirlwall, M.F., 1995. Low-pressure evolution of magmas from the Călimani, Gurghiu and Harghita Mountains, East Carpathians. *Acta Vulcanologica* 7, 43–52.
- Mason, P.R.D., Downes, H., Thirlwall, M.F., Seghedi, I., Szakács, A., Lowry, D., Matthey, D., 1996. Crustal assimilation as a major petrogenetic process in the East Carpathian Neogene and Quaternary continental margin arc, Romania. *Journal of Petrology* 37, 927–959.
- Mason, P.R.D., Seghedi, I., Szakács, A., Downes, H., 1998. Magmatic constraints on geodynamic models of subduction in the East Carpathians, Romania. *Tectonophysics* 297, 157–176.
- Mațenco, L., Bertotti, G., 2000. Tertiary tectonic evolution of the external East Carpathians (Romania). *Tectonophysics* 316, 255–286.
- Mațenco, L., Kręzek, C., Merten, S., Cloetingh, S., Andriessen, P., 2010. Characteristics of collisional orogens with low topographic build-up: an example from the Carpathians. *Terra Nova* 22, 155–165.
- McLeod, C.L., Davidson, J.P., Nowell, G.M., de Silva, S.L., 2012. Disequilibrium melting during crustal anatexis and implications for modeling open magmatic systems. *Geology* 40, 435–438.
- Miyashiro, A., 1974. Volcanic rock series in island arcs and active continental margins. *American Journal of Science* 274, 321–355.
- Nash, W.P., Crecraft, H.R., 1985. Partition coefficients for trace elements in silicic magmas. *Geochimica et Cosmochimica Acta* 49, 2309–2322.
- Nițoi, E., Munteanu, M., Marinca, S., Paraschivoiu, V., 2002. Magma-enclaves interaction in the East Carpathians subvolcanic zone, Romania: petrogenetic implications. *Journal of Volcanology and Geothermal Research* 118, 229–259.
- Papp, D.C., Ureche, I., Seghedi, I., Downes, H., Dallai, L., 2005. Petrogenesis of convergent-margin calc-alkaline rocks and the significance of the low oxygen isotope ratios: the Rodna-Bărgău neogene subvolcanic area (Eastern Carpathians). *Geologica Carpathica* 56, 77–90.
- Pécskay, Z., Edelstein, O., Seghedi, I., Szakács, A., Kovacs, M., Crihan, M., Bernad, A., 1995. K-Ar datings of Neogene volcanic rocks of the Neogenic-Quaternary calc-alkaline volcanic rocks in Romania. *Acta Vulcanologica* 7, 53–61.
- Pécskay, Z., Lexa, J., Szakács, A., Seghedi, I., Balogh, K., Konečný, V., Zelenka, T., Kovacs, M., Póka, T., Fülöp, A., Márton, E., Panaiotu, C., Cvetković, V., 2006. Geochronology of Neogene-Quaternary magmatism in the Carpathian arc and Intra-Carpathian Area: a review. *Geologica Carpathica* 57, 511–530.
- Pécskay, Z., Seghedi, I., Kovacs, M., Szakács, A., Fülöp, A., 2009. Geochronology of the Neogene calc-alkaline intrusive magmatism in the “Subvolcanic Zone” of the Eastern Carpathians (Romania). *Geologica Carpathica* 60, 181–190.
- Peltz, S., Vasiliu, C., Udrescu, C., 1972. Petrology of igneous rocks from the Neogene East Carpathian subvolcanic zone. *Anuarul Institutului de Geologie și Geofizică* 39, 177–218 (in Romanian).
- Prelević, D., Seghedi, I., 2013. Magmatic response to the post-accretionary orogenesis within Alpine-Himalayan belt – preface. *Lithos* 180–181, 1–4.
- Ridolfi, F., Renzulli, A., Puerini, M., 2010. Stability and chemical equilibrium of amphibole in calc-alkaline magmas: an overview, new thermobarometric formulations and application to subduction-related volcanoes. *Contributions to Mineralogy and Petrology* 160, 45–66.
- Rudnick, R.L., Gao, S., 2003. Composition of the continental crust. In: Rudnick, R.L. (Ed.), *Treatise on Geochemistry/The Crust* vol. 3. Elsevier, Amsterdam, pp. 1–64.
- Săndulescu, M., 1994. Overview on Romanian geology. II Alcpa congress field guidebook. *Romanian Journal of Tectonics and Regional Geology* 75, 3–15.
- Schmid, S.M., Bernoulli, D., Fügenschuh, B., Mațenco, L., Schefer, S., Schuster, R., Tischler, M., Ustaszewski, K., 2008. The Alpine-Carpathian-Dinaride orogenic system: correlation and evolution of tectonic units. *Swiss Journal of Geosciences* 101, 139–183.
- Seghedi, I., Downes, H., 2011. Geochemistry and tectonic development of Cenozoic magmatism in the Carpathian-Pannonian region. *Gondwana Research* 20, 655–672.
- Seghedi, I., Szakács, A., Mason, P.R.D., 1995. Petrogenesis and magmatic evolution in the East Carpathian Neogene volcanic arc (Romania). *Acta Vulcanologica* 7, 135–143.
- Seghedi, I., Downes, H., Szakács, A., Mason, P.R.D., Thirlwall, M.F., Roșu, E., Pécskay, Z., Márton, E., Panaiotu, C., 2004. Neogene-Quaternary magmatism and geodynamics in the Carpathian-Pannonian region: a synthesis. *Lithos* 72, 117–146.
- Seghedi, I., Szakács, A., Pécskay, Z., Mason, P.R.D., 2005. Eruptive history and age of magmatic processes in the Călimani volcanic structure. *Geologica Carpathica* 56, 67–75.
- Seghedi, I., Mațenco, L., Downes, H., Mason, P.R.D., Szakács, A., Pécskay, Z., 2011. Tectonic significance of changes in post-subduction Pliocene-Quaternary magmatism in southeast part of the Carpathian-Pannonian region. *Tectonophysics* 502, 146–157.
- Shinjo, R., Ginoza, Y., Meshesha, D., 2010. Improved method for Hf separation from silicate rocks for isotopic analysis using Ln-spec resin column. *Journal of Mineralogical and Petrological Sciences* 105, 297–302.
- Sisson, T.W., 1994. Hornblende-melt trace-element partitioning measured by ion microprobe. *Chemical Geology* 117, 331–344.
- Sisson, T.W., Bacon, C.R., 1992. Garnet/high-silica rhyolite trace element partition coefficients measured by ion microprobe. *Geochimica et Cosmochimica Acta* 56, 2133–2136.
- Sun, S.-s., McDonough, W.F., 1989. Chemical and isotopic systematics of oceanic basalts: implications for mantle compositions and processes. In: Saunders, A.D., Norry, M.J. (Eds.), *Magmatism in the Ocean Basins*. Geological Society of London Special Publications Vol. 42, pp. 313–345.
- Sylvester, P.J., 1998. Strongly peraluminous granites. *Lithos* 45, 29–44.
- Szakács, A., Pécskay, Z., Silye, L., Balogh, K., Vlad, D., Fülöp, A., 2012. On the age of the Dej Tuff, Transylvanian Basin, Romania. *Geologica Carpathica* 63, 138–148.
- Tari, G., Dövényi, P., Dunkl, I., Horváth, F., Lenkey, L., Ștefănescu, M., Szafián, P., Tóth, T., 1999. Lithospheric structure of the Pannonian basin derived from seismic, gravity

- and geothermal data. In: Durand, B., Jolivet, L., Horváth, F., Sérranne, M. (Eds.), *The Mediterranean Basins: Tertiary Extension within the Alpine Orogen*. Geological Society of London Special Publications Vol. 156, pp. 215–250.
- Tischler, M., Gröger, H.R., Fügenschuh, B., Schmid, S.M., 2007. Miocene tectonics of the Maramures area (northern Romania): implications for the mid-Hungarian fault zone. *International Journal of Earth Sciences* 96, 473–496.
- Tischler, M., Mațenco, L., Filipescu, S., Gröger, H.R., Wetzel, A., Fügenschuh, B., 2008. Tectonics and sedimentation during convergence of the ALCAPA and Tisza-Dacia continental blocks: the Pienide nappe emplacement and its foredeep (N. Romania). In: Siegesmund, S., Fügenschuh, B., Froitzheim, N. (Eds.), *Tectonic Aspects of the Alpine-Dinaride-Carpathian System*. Geological Society of London Special Publications Vol. 298, pp. 317–334.
- Zindler, A., Hart, S., 1986. Chemical Geodynamics. *Annual Review of Earth and Planetary Sciences* 14, 493–571.